Article

Cell Chemical Biology

Discovery of MARK2 as a physiological kinase for PER2 in the mammalian clock

Graphical abstract

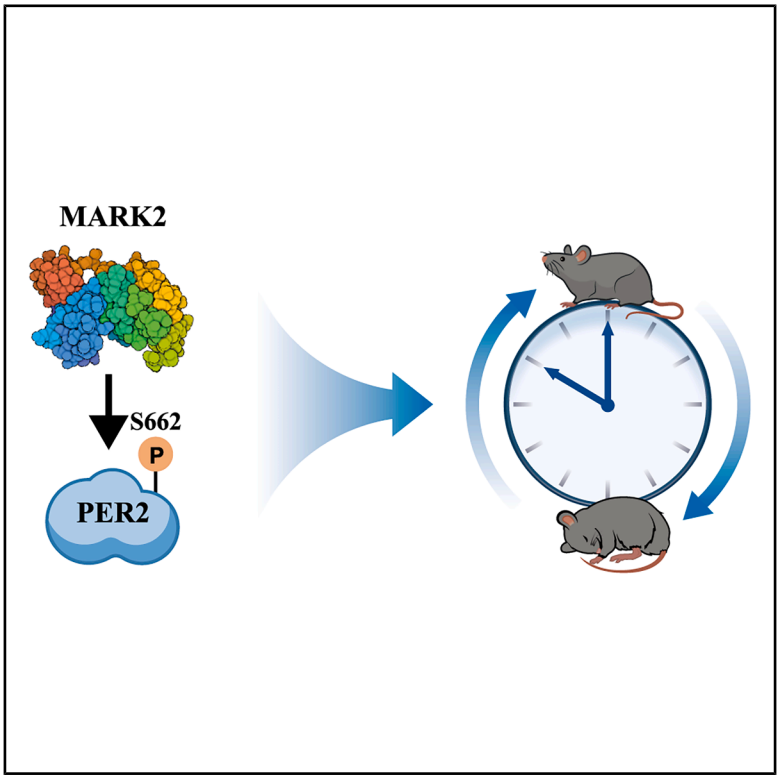

Authors

Yuxiang Liu (刘玉祥), Yang Li (李扬), Tenghui Yu (余腾辉), ..., Shangchen Liu (刘尚臣), Juan Huang (黄娟), Yi Rao (饶毅)

Correspondence

yrao@pku.edu.cn

In brief

Phosphorylation of PER2 at serine 662 regulates circadian timing, and its serine to glycine G (S662G) mutation causes familial advanced sleep phase syndrome. Liu et al. identify MARK2 as the physiological S662 kinase through biochemical purification. MARK2 stabilizes PER2 to regulate the circadian rhythm, and its loss in mice exhibits phase advancement and period shortening.

Highlights

- Biochemical purification identifies MARK2 as a PER2 S662 kinase
- MARK2-mediated phosphorylation stabilizes PER2
- MARK2 regulates cellular circadian period in an S662-dependent manner
- Neuronal knockout of MARK2 in mice shortens period and advances activity phase

Liu et al., 2026, Cell Chemical Biology *33*, 379–395
March 19, 2026
https://doi.org/10.1016/j.chembiol.2026.02.007

CellPress

Cell Chemical Biology

CellPress

Article

Discovery of MARK2 as a physiological kinase for PER2 in the mammalian clock

Yuxiang Liu (刘玉祥),[1,2,3,4,5,7] Yang Li (李扬),[1,2,3,4,5,7] Tenghui Yu (余腾辉),[3,4,5,7] Tao V. Wang (王涛),[3,4,5,7] Yunfeng Cui (崔云凤),[3,4,5] Chen Zhu (朱晨),[3,4,5] Xiaobo Jia (贾晓波),[1,2] Chenggang Li (李成钢),[1,2,3,4,5] Yuxin Shen (沈雨欣),[1,2] Zhun Wang (王准),[1,2] Shangchen Liu (刘尚臣),[1,2] Juan Huang (黄娟),[1,2] and Yi Rao (饶毅)[1,2,3,4,5,6,8,*]

[1]Chinese Institute for Brain Research, Beijing (CIBR), Beijing, China

[2]Chinese Institutes for Medical Research, Beijing (CIMR), Capital Medical University, Beijing, China

[3]Laboratory of Neurochemical Biology, Peking-Tsinghua Center for Life Sciences, Peking-Tsinghua-NIBS (PTN) Graduate Program, School of Life Sciences, Beijing, China

[4]Department of Chemical Biology, College of Chemistry and Chemical Engineering, Beijing, China

[5]School of Pharmaceutical Sciences, PKU-IDG/McGovern Institute for Brain Research, Peking University, Beijing, China

[6]SANS Center for AI Therapeutics and Department of Pharmacology, School of Basic Medical Sciences, Fudan University Shanghai Medical College, Shanghai, China

[7]These authors contributed equally

[8]Lead contact

*Correspondence: yrao@pku.edu.cn

https://doi.org/10.1016/j.chembiol.2026.02.007

SIGNIFICANCE The circadian clock regulates daily rhythms in physiology and behavior, and its disruption is associated with sleep disorders and other health problems. PERIOD2 (PER2) is a core molecular regulator of the circadian clock and a human mutation was discovered in 2001 in the PER2 gene changing the serine 662 to glycine (S662G) residue in PER2 protein causes familial advanced sleep phase (FASP) syndrome with phase advancement and period shortening. This mutation abolishes the phosphorylation of S662, a modification that acts as a molecular switch to stabilize PER2 and prolong circadian period. There has been much interests in identifying kinases phosphorylating S662 over the past quarter century. Here, after biochemical purification, we identified microtubule affinity-regulating kinase 2 (MARK2), an AMPK-related kinase (ARK), as a PER2 S662 kinase. Further examination of all 21 ARKs detected that some of them phosphorylated PER2 S662. MARK2 directly phosphorylates PER2, binds to PER2 and delays its degradation through S662 phosphorylation. Genetic deletion of MARK2 gene from cultured human cells led to shortened circadian rhythm, and this phenotype was dependent on PER2 S662. Specific deletion of the MARK2 gene from neurons in the mouse brain caused phase advancement and period shortening. Our work not only identifies MARK2 as a physiologically significant regulator of the circadian clock, but also highlights the effectiveness of biochemical approaches in solving physiological puzzles, and suggests possible involvement of ARKs in the clock by regulating phosphorylation of PER2 and other proteins.

SUMMARY

Genetics has been a powerful approach in studying the circadian clock, uncovering the first gene *Period* (*Per*) as a key regulator. Human mutation in serine 662 (S662) was found in 2001 to cause familial advanced sleep phase (FASP) syndrome with phase advancement and period shortening. We found S662 phosphorylation by casein kinase 1 (CK1) δ and ε, testis-specific serine kinase (TSSK) 1 and 2, and salt inducible kinase (SIK) 1–3, but no phase advancement phenotype after genetic deletion of any of these seven genes. Our biochemical purification revealed microtubule affinity regulating kinase 2 (MARK2) in phosphorylating S662, binding to and stabilizing PER2. Circadian period was shortened in *Mark2*-deficient cells in an S662-dependent manner. Neuronal specific *Mark2* knockout mice showed phase advancement and period shortening. We have discovered MARK2 as a physiologically significant regulator of the clock, and shown the effectiveness of biochemical purification in mechanistic studies of behaviors.

INTRODUCTION

Circadian rhythm is important for basic physiology and its abnormalities have health implications. With more than a billion cross-time zone travelers per year and approximately 20% of Western workers taking shift work,[1] health problems associated with disturbances of the circadian rhythm are of potential concerns.[2–7]

The circadian clock is an intrinsic timing system driving the daily rhythm of multiple systems such as the sleep/wake cycle, immune responsiveness and metabolism.[8–10] In mammals, the master clock resides in the hypothalamic suprachiasmatic nucleus (SCN), which synchronizes circadian oscillations in cells throughout the body.[11,12] More than 50 years ago, the genetic approach has made breakthroughs in our understanding of the molecular mechanisms of the circadian clock with discoveries of genetic mutations affecting the clock in *Drosophila*,[13] *Neurospora*,[14] and *Chlamydomonas*.[15] Since then, genetic studies in multiple organisms, especially *Drosophila* and mice, have established an interlocked transcription-translational feedback loop (TTFL) as the underlying molecular mechanisms of the circadian clock in animals.[16–24]

The first key gene found to be conserved from flies to humans is *Period* (*Per*).[13] In mammals, the first TTFL involves the transcriptional activation of three period genes *Per* and two cryptochrome (*Cry*) genes by BMAL1 and CLOCK, while PER and other proteins form macromolecular complexes to repress their transcription.[19,25–36] The second TTFL involves the activation of two nuclear receptor genes (*Rorα/β*, *Rev-erbα*) by Bmal1 and Clock, while Rorα/β and Rev-erbα feedback on *Bmal1* transcription.[37] More recently, a nucleotide triphosphatase (NTPase) has been proposed to be conserved across all eukaryotes in circadian regulation.[38]

Among the core clock proteins, the PER family exhibits the most robust circadian oscillations in protein abundance.[39–41] After synthesis, PER2 proteins undergo progressive phosphorylation at multiple sites to regulate their stability, repressor activity, and subcellular localization.[33,34,36,41–46] Two key phosphorylation clusters regulate PER2 dynamics: the S478/482 phosphodegron (in mouse), whose phosphorylation recruits the E3 ubiquitin ligase β-TrCP to promote PER2 degradation, thereby accelerating the circadian cycle; and the FASP region (starting at S659 in mouse or S662 in human), a cluster of five serines (SxxSxxSxxSxxS), whose phosphorylation stabilizes PER2 and prolongs the circadian period by inhibiting phosphodegron phosphorylation.[33,41–44,47–56] Phosphorylation of S662 serves as the priming event for subsequent phosphorylation within the FASP region.[41,51,57–59] The S662G mutation in human abrogates this priming phosphorylation, prevents subsequent FASP phosphorylation[41,48,51,60] and causes familial advanced sleep phase syndrome with a ∼4 h shorter circadian period, a phenotype replicated in transgenic mice.[43,48]

A 2001 report presented results of human genetic studies in a family showing a point mutation converting serine (Ser) to glycine (Gly) at the 662th amino acid (aa) residue in the human PER2 protein (hPER2) to correlate with the familial advanced sleep phase syndrome (FASPS).[43,61] hPER2 S662 was a priming site for casein kinase 1δ (CK1δ).[43,51,57,58] CK1δ and CK1ε have been proposed to act as a critical phosphoswitch in PER2 phosphorylation and could phosphorylate mouse PER2 on at least three regions: the PER2-phosphodegron (S478),FASP priming sites (S659) and downstream serines within the FASP region.[33,50–52,62] CK1δ/ε form stable complexes with PER2 and switch their substrate preference via conformational changes in their activation loop and alterations in the phosphorylation status of their C-terminal tail, conferring a switch-like behavior in regulation of PER2 phosphorylation.[33,34,36,56–59,63] However, when both *CK1δ* and *CK1ε* were knockout in HEK293 cells, the phosphorylation level of S662 was markedly reduced but not abolished, suggesting existence of additional kinases for this site.

In a long-term effort to search for kinases upstream of hPER2, we have tried a molecular biological and a biochemical approach for 14 years. Before the availability of specific antibodies for the phosphorylated S662 of hPER2, we co-transfected complementary DNAs (cDNAs) for protein kinases in the human kinome with hPER2, and found several kinases phosphorylating fragments of hPER2. After the availability of a monoclonal antibody (mAb) recognizing the S662 phosphorylated form of hPER2, we confirmed phosphorylation of PER2 S662 by CK1 δ and ε, testis specific serine kinases (TSSKs) 1 and 2. Of all the CK1s, only CK1δ and ε, but not CK1γ1, 2 or 3, could phosphorylate S662 *in vitro*. Genetic knockout (KO) of *CK1 δ* and ε in the human D15 cell line showed phase delay, not advancement. The second approach was biochemical purification with the anti-phospho-S662-hPER2 as the monitor, leading to our discovery of microtubule activity regulatory kinases (MARKs) 2 and 3 as S662 kinases. They belong to the subfamily of adenosine monophosphate (AMP)-activated protein kinase (AMPK) related kinases (ARKs).[64–76] We compared the *in vitro* activities of all ARKs and found that SIK 1–3, MARK 1–4, TSSK1 and 2 could phosphorylate PER2-S662, with MARK2 and MARK3 being the strongest. Genetic KO of *SIKs* showed no circadian phase advancement phenotype.[77–79] We generated KO of *TSSK 1* and *2* (including their double KO) in mice and found no circadian phase advancement phenotype. Thus, the circadian phenotype of *CK1s*, *SIKs*, and *TSSKs* knockout mice were not consistent with the circadian phenotype of human FASPS patients[48] or *PER2 S662G* mutant mice[43] *in vivo*.

Over-expression of *MARK2* or *3* lengthened the period while KO of *MARK2* but not *MARK3* shortened the period in cultured cells, similar to *S662G* mutation. Further biochemical and genetic evidence in cultured cells support that MARK2 is both biochemically and physiologically upstream of hPER2-S662. In mice, neuronal KO of *MARK2* led to phase-advancement and period shortening, whereas *MARK3* KO, *MARK3* neuronal specific KO and *MARK4* neuronal specific KO mice exhibited no abnormality in circadian rhythm. Thus our long time search for PER2 S662 kinases has uncovered MARK2 as a kinase of physiological significance in clock regulation.

RESULTS

CK1 δ and ε phosphorylation of hPER2 S662 and circadian rhythm

Several labs have published that CK1δ and CK1ε could phosphorylate PER2.[41,48,62,80] They were once thought to phosphorylate S662 of PER2,[46] a suggestion later rejected by the same

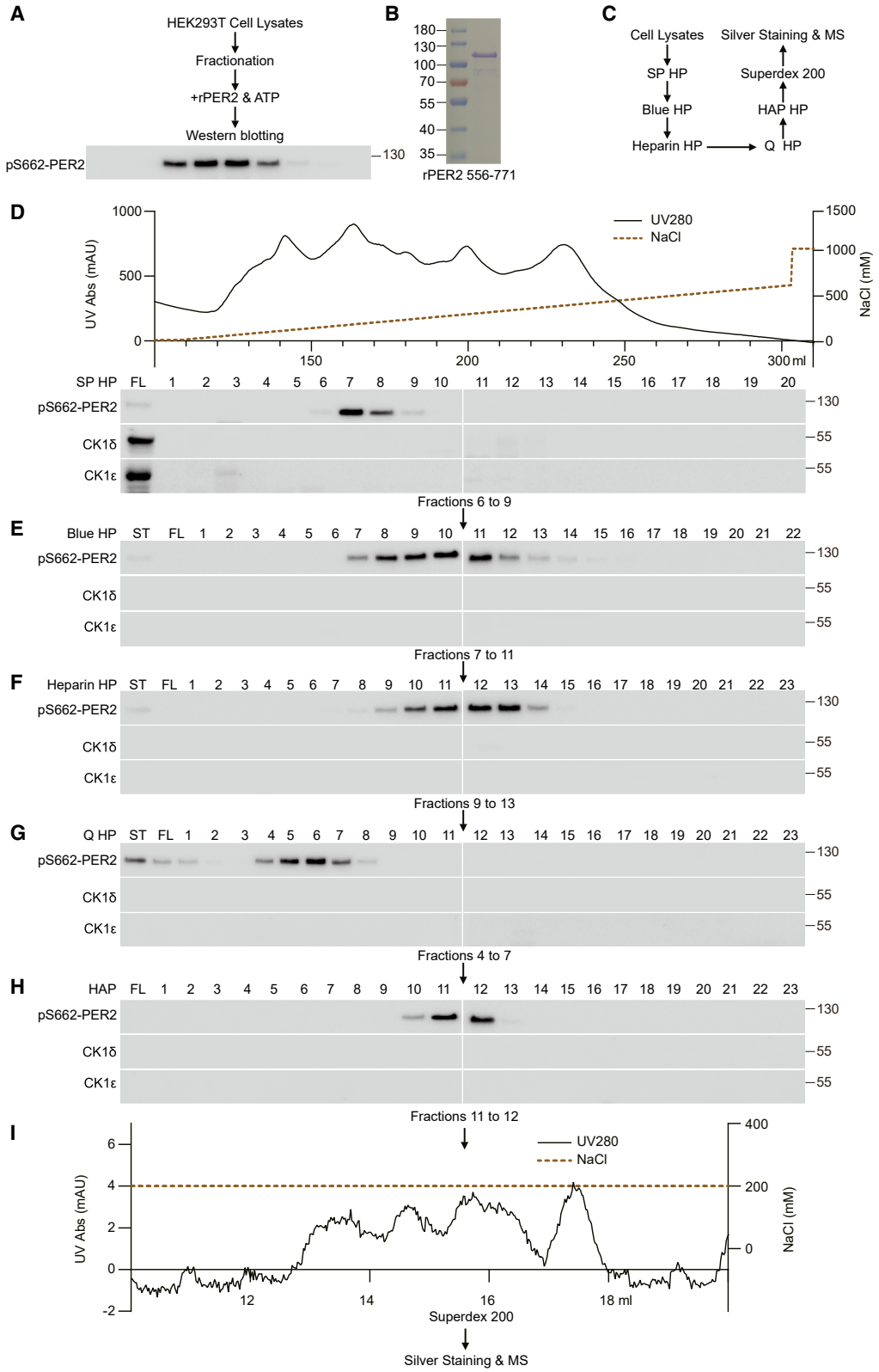

Figure 1. Biochemical purification of PER2 662 phosphorylating activities from HEK293 cells

(A) A diagram of detection of hPER2 S662 phosphorylating activities in fractions of HEK293 cell extracts. Each fraction was incubated with 1 μg recombinant PER2 556-771 (rPER2 556–771) and 1 mM ATP for 1 h, followed by immunoblotting with a phospho-S662-specific antibody.

(legend continued on next page)

researchers when they failed to detect direct phosphorylation of S662 in a peptide of 19 aa residues from PER2.[43] This contradiction was later resolved by Narasimamurthy et al. (2018), who confirmed direct S662 phosphorylation by CK1δ/ε.[51] Recent structural and biochemical studies have elucidated the underlying mechanism: conformational switch in the CK1 activation loop governs substrate selectivity for the PER2 phosphoswitch, and phosphorylation of the PER2 FASP region in turn allosterically inhibits CK1 activity, ensuring precise control of the circadian period.[53,54,56–59]

Our early efforts were carried out prior to the availability of antibodies recognizing human PER2 phosphorylated at 662 (phospho-S662). We screened a cDNA library of 288 human kinases (Table S1) for their abilities to phosphorylate six hPER2 fragments using Phos-tag to detect phosphorylation-induced gel shifts in sodium dodecyl sulfate-polyacrylamide gel electrophoresis (SDS-PAGE).[81] Co-transfection of kinase cDNAs with hPER2 fragments in HEK293T cells revealed several kinases capable of phosphorylating specific PER2 regions. Fragment 1–200 was not phosphorylated by any of the kinases screened. Cyclin dependent kinase 5 (CDK5) phosphorylated fragment 150–400. cAMP-dependent protein kinase catalytic subunit beta (PRKACB), cGMP-dependent protein kinase 1 (PRKG1) and inhibitor of nuclear factor kappa-B kinase subunit β (IKKβ) phosphorylated Fragment 328–556. CK1δ and CK1ε, TSSK2 and IKKε phosphorylated fragment 556–771. The last fragment contains S662. To clarify whether CK1δ and CK1ε could phosphorylate S662 of hPER2, we first obtained a mAb against phospho-S662 hPER2. This antibody specifically recognized phosphorylated wild-type (WT) human or mouse PER2 (hPER2 or mPER2), but not their mutants with serine to alanine (A) or serine to aspartic acid (D) (S662A/S662D in hPER2 or S659A/S659D in mPER2) mutants (Figures S1A–S1C). Recognition was abolished by phosphatase treatment (Figures S1A–S1C).

Using this antibody, we confirmed that CK1δ and CK1ε phosphorylated hPER2 at S662 *in vitro* (Figures S1D–S1H). FLAG-tagged CK1δ (Figure S1D) or CK1ε (Figure S1E) phosphorylated S662 of hPER2 556–771 in HEK293 cells. Transfection of increasing amounts of *CK1δ* or *CK1ε* plasmids increased phosphorylation of hPER2 at S662 (Figure S1G). Other CK1 family members (CK1α1, α2, γ1, γ2, γ3) were also tested either upon transfection of their FLAG-tagged forms into HEK cells (Figure S1F) or with *in vitro* kinase assays with immunoprecipitated CK1 proteins and recombinant hPER2 fragments (556–771) (Figure S1H). None of these CK1s phosphorylated S662 of PER2.

Because full-length CK1δ/ε are autoinhibited by C-terminal autophosphorylation, we expressed their truncated (1–317) variants in *Escherichia coli* (*E. coli*) to confirm direct phosphorylation. Recombinant CK1δ 1–317 (Figures S2A, S2B, S2E, and S2G) and CK1ε 1–317 (Figures S2C, S2D, S2F, and S2G), but not other CK1s (Figures S2G and S2J), phosphorylated bacterially expressed hPER2 556–771 S662. The Michaelis-Menton constant (Km) of CK1δ on PER2-S662 321–771 was 6.58 ± 1.71 μM (Figure S2H) and that for CK1ε was 7.38 ± 1.61 μM (Figure S2I).

To investigate the function roles of *CK1δ* and *CK1ε* in regulating circadian rhythm, we first used *Per2-dLuc* cells (D15 cells), a human U2OS cell line with *Per2* promoter driven expression of luciferase (*Per2::luciferase*) reporting the circadian clock (Figure S3C).[82] Genetic knockout of *CK1δ* (Figure S3A) or *CK1ε* (Figure S3B) in D15 cells significantly increased the length of circadian period (Figures S3C and S3D), consistent with a previous report.[35]

We then used genetically targeted mice to investigate the physiological function of *CK1δ*. Neuronal specific-conditional knockout *CK1δ* mice also resulted in a lengthened circadian period by 0.3 h (Figures S3E and S3F). Our results (Figures S1–S3) are consistent with others that, although CK1δ and CK1ε could phosphorylate S662 in PER2 *in vitro*, elimination of *CK1δ* and *CK1ε* from human cell lines or mice caused phase lengthening.[35,36,41,43,50,54,57,83–88] Furthermore, when both *CK1δ* and *CK1ε* were knockout in HEK293 cells (Figures S3A and S3B), the kinase activities for S662 was reduced, but not eliminated (Figures S3G and S3H), suggesting existence of additional kinases for this site.

TSSK 1 and 2 phosphorylation of hPER2 S662 and the circadian rhythm *in vivo*

Our initial cDNA screen also found TSSK2 as a kinase for the PER2 556–771 fragment. We co-transfected cDNAs encoding TSSK family kinases with hPER2 556–771 in HEK293T cells and found PER2-S662 phosphorylation by TSSK1 and TSSK2 but not by TSSK 3, 4, or 6 (Figure S4A). Increasing concentrations of cDNAs for *TSSK1* and *TSSK2* in HEK cells led to increased phosphorylation of PER2-S662 (Figure S4B).

To determine the physiological relevance of *Tssks* in circadian regulation, we generated *Tssk2* knockout mice (Figure S4C) and *Tssk1-Tssk2* conditional double knockout mice (*Tssk1-Tssk2*^{flox}, Figure S4D). Neither *Tssk2* single KO (Figures S4E–S4H) nor neuronal *Tssk1*;*Tssk2* double KO mice (Figures S4I–S4L) exhibited any circadian phenotype.

Discoveries of MARK2 and MARK3 as PER2 S662 kinases via biochemical purification

Given the persistence of some S662 phosphorylation in *CK1δ/ε* double knockout (DKO) cells, we carried out biochemical purification of kinase(s) whose activities were monitored by the anti-phospho-S662 mAb (Figure 1A). We used extracts from 50 L of

(B) Coomassie blue staining of MBP-hPER2 556-771-GFP-8His substrate purified from *E. coli*. rPER2 was used with the same amount for each phosphorylation assay.
(C) Overview of the six-step chromatographic purification strategy for PER2 S662 kinase. Approximately 50L of suspension-cultured HEK cells were used as the starting material, and six chromatographic columns were tested with a 10% equivalent of the starting material for purification of the activity before all materials were used.
(D) PER2 S662 phosphorylating activities in SP HP column. Strong PER2 S662 phosphorylating activities were detected in fractions 7 and 8, whereas CK1δ and CK1ε were only detected in flow-through fractions.
(E–I) PER2 S662 phosphorylating activities from SP HP columns (fraction 7 and 8) were purified in the next five sequentially connected chromatography steps in the order of blue HP (E), heparin HP (F), Q HP (G), HAP (H), and Superdex 200 (I). Active fractions from each column were pooled and loaded onto the next column.
See also Figures S1–S4 and Table S1.

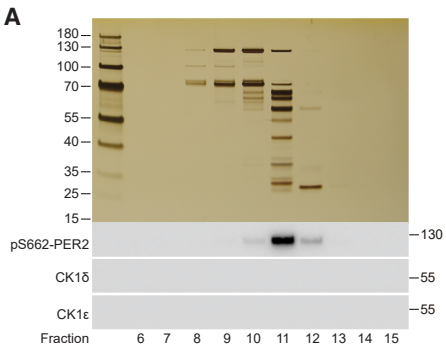

B

Protein	Mascot score	AA (amino acid)	MW	Matched peptides
MARK3	24.101	753	84429	5
MARK2	22.977	788	87911	6
GSK3β	4.719	420	46744	3
MKNK1	3.242	465	51342	2
SRC	3.078	536	59853	3
RSK2	1.065	740	83736	1

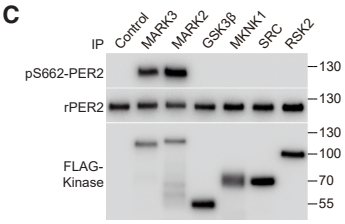

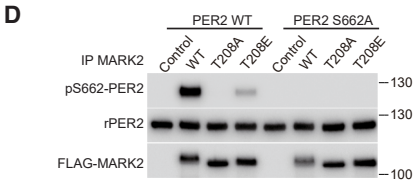

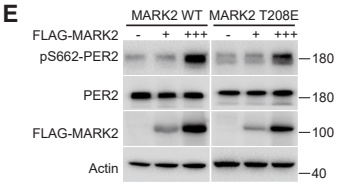

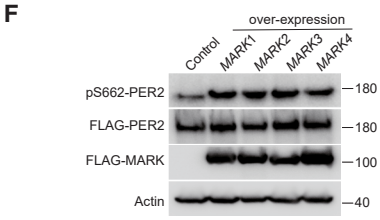

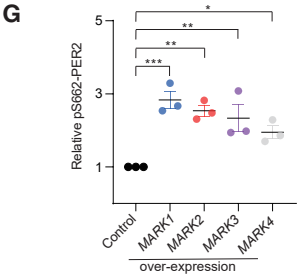

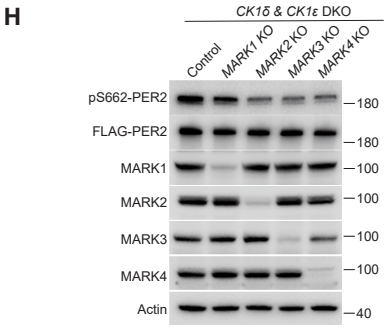

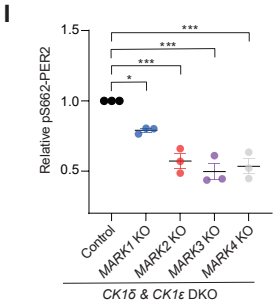

Figure 2. PER2 S662 phosphorylation by MARK 2 and 3

(A) Silver staining and PER2 S662 phosphorylation assay of the fractions from the final Superdex 200 column. Phosphorylating activity was detected in fraction 11 and isolated for MS.

(B) Six kinases were identified by MS, ranked from the highest to lowest Mascot scores. SRC is a tyrosine-protein kinase and the others are serine/threonine kinases.

(C) hPER2 S662 was phosphorylated *in vitro* by immunoprecipitated MARK 2 and 3 but not by GSK3β, MKNK1, SRC, or RSK2. FLAG-tagged kinases were expressed in HEK293 cells, immunoprecipitated, and assayed with recombinant hPER2 (556–771).

(D) rPER2 S662 were phosphorylated *in vitro* by WT MARK2 or T208E but not its T208A mutant immunoprecipitated from HEK cells.

(E) MARK2 WT and its T208E mutant increased PER2 S662 phosphorylation levels in a dose-dependent manner. HEK293T cells were co-transfected with increasing concentrations of cDNAs for MARK2. After 24 h of culture, cells were harvested and lysed for western analysis.

(F) Over-expression (OE) of each MARK family member (MARK1-4) in HEK cells increased PER2 S662 phosphorylation.

(G) Quantification of (F) by ImageJ (n = 3 independent biological replicates).

(H) Individual KO of *MARK* genes in *CK1δ/ε* double-KO HEK293 cells reduced PER2 S662 phosphorylation.

(I) Quantification of (H) by ImageJ (n = 3 independent biological replicates). One ANOVA followed by Dunnett's multiple comparisons test (G and I); data are presented as mean ± SEM. See also Figure S5.

HEK293T cells (2.0–3*10^6 cells/mL) cultured in suspension as the starting material (Figure 1A), the recombinant hPER2 556–771 purified from *Escherichia coli* (*E. coli*) as the substrate (Figure 1B). Six chromatographic columns (SP HP, blue HP, heparin HP, Q HP, HAP, and Superdex 200) were tested with a 10% equivalent of the starting material for purification of the activity before all materials were used (Figure 1C). At every step, hPER2-S662 phosphorylation was monitored in an aliquot from each fraction. Lysates with 500 mg proteins (in a concentration of 10 mg/mL) were fractionated by a 10 mL SP HP column and eluted with a gradient of NaCl. Strong PER2 S662 phosphorylating activities were detected in fractions 7 and 8 (210–240 mM NaCl) while CK1δ and CK1ε were only detected in flow-through fractions (0 mM NaCl) (Figure 1D). Active fractions from each column were pooled and loaded onto the next column: fractions 7 to 11 (1,050–1,650 mM NaCl) from the Blue column (Figure 1E), fractions 9 to 13 (270–330 mM NaCl) from the Heparin column (Figure 1F), fractions 4 to 7 (120–210 mM NaCl) from the Q HP column (Figure 1G), fractions 11 to 12 (150–180 mM K_2PO_4) from the HAP column (Figure 1H). Fractions 11 and 12 (150–180 mM K_2PO_4) from the HAP column were fractionated by Superdex 200 column and eluted with a 200 mM NaCl (Figure 1I).

Fractions from the Superdex 200 column were dialyzed, run onto a polyacrylamide gel and silver-stained (Figure 2A). We excised all bands from fraction 11 in the silver-stained gel and analyzed their contents by mass spectroscopy (MS). We detected 6 protein kinases: MARK3, MARK2, GSK-3β, MKNK1, SRC, and RSK2 (Figure 2B).

Phosphorylation of hPER2 S662 by MARKs and 3

We expressed each of the above kinases in HEK cells with an FLAG epitope fused in frame to their N termini (Figure 2C).[89] Each FLAG-tagged kinase was immunoprecipitated from HEK

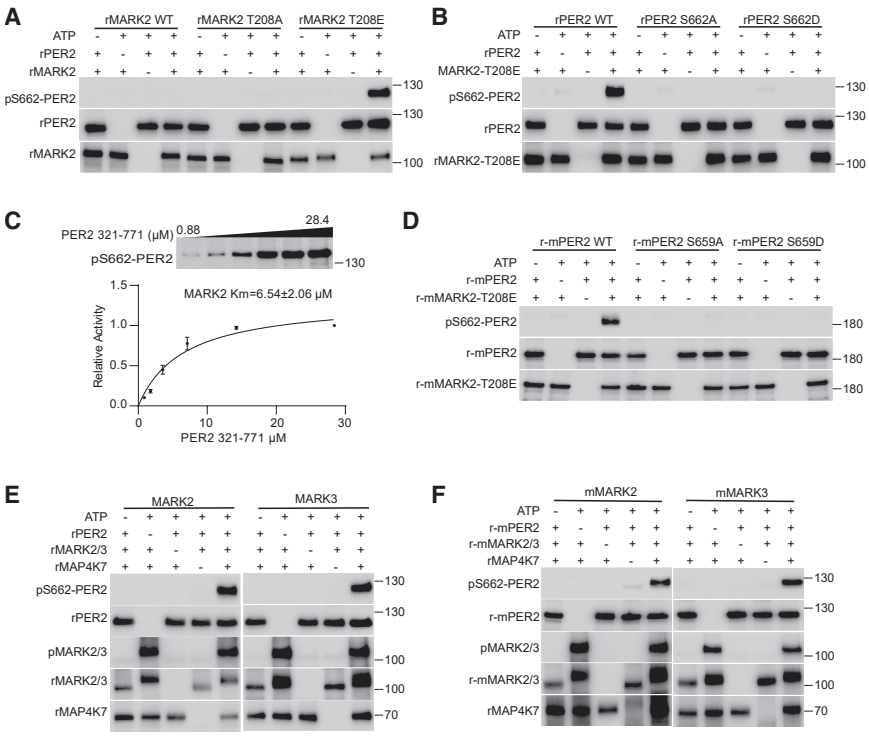

Figure 3. Direct phosphorylation of PER2 S662 by recombinant MARK2

All experiments in this figure were performed with recombinant proteins expressed in *E. coli*. The hPER2 (rPER2 WT, S662A, S662D) and mouse (r-mPER2 WT, S659A, S659D) substrates comprise residues 556–771. rMARK2 was a recombinant human MARK2 protein expressed in *E. coli*. rMAP4K7 was recombinant human MAP4K7 (1–500 aa).

(A and B) Recombinant MARK2 T208E, but not WT or T208A, directly phosphorylated hPER2 at S662, but not the S662A or S662D mutants.

(C) Km of recombinant MARK2 T208E on PER2. About 0.2 μg rMARK2 T208E was incubated with the recombinant rPER2 321–771 of different concentrations at 37°C for 30 min. Western blots were quantified by the ImageJ (n = 3 independent biological replicates) and Km was calculated by the GraphPad software. Data are presented as mean ± SEM.

(D) Recombinant mouse MARK2 T208E phosphorylated mouse PER2 at S659.

(E) Recombinant WT MARK 2 or 3, pre-activated by rMAP4K7, could phosphorylate recombinant hPER2 S662. MAP4K7 is an upstream kinase for the MARKs. Recombinant MARKs purified from *E. coli* were incubated with MAP4K7 for 1 h before being tested for their activities on recombinant hPER2. MARK2/3 activation was confirmed by detecting phosphorylation of the MARK activation loop with an anti-phospho-MARK2/3 antibody.

(F) MAP4K7 pre-treatment activated recombinant mouse MARK2 and MARK3 to phosphorylate mPER2 S659. See also Figure S6.

cells and tested for phosphorylation of recombinant hPER2 556–771 purified from *E. coli*. While GSK-3β, MKNK1, SRC and RSK2 were unable to phosphorylate hPER2-S662, MARKs 2 and 3 robustly phosphorylated hPER2-S662 (Figure 2C). If S662 in PER2 was mutated to A, it could not be phosphorylated by either MARK2 (Figure 2D) or MARK3 (Figure S5A).

MARK2 and MARK3 are activated by phosphorylation of a conserved threonine residue within their activation loop (T208 in MARK2, T211 in MARK3). If threonine 208 (T208) in MARK2 (Figure 2D) or T211 in MARK3 (Figure S5A) was mutated to A, PER2-S662 could not be phosphorylated by the mutated kinase. T208 mutation to glutamate (E) of MARK2 (Figure 2D) or T211E of MARK3 (Figure S5A) decreased their activities. Increasing concentrations of cDNAs for wild type (WT) or T208E mutant MARK2 (Figure 2E) or WT or T211E-MARK3 (Figure S5B) transfected into HEK cells led to increased phosphorylation of hPER2-S662 in HEK cells. Mouse MARK2 and 3 were also able to phosphorylate hPER2-S662 (Figures S5C and S5D).

The MARK family comprises four members (MARKs 1–4). Over-expression of any of the four MARKs in HEK cells enhanced PER2 S662 phosphorylation (Figures 2F and 2G). When *MARK 1*, *2*, *3*, or *4* was individually knocked-out in *CK1δ* and *CK1ε* double KO HEK293 cells, the phosphorylation of PER2 S662 was reduced by 21%, 43%, 50%, and 47%, respectively (Figures 2H and 2I). When all four *MARKs* were knocked-out in HEK293 cells (Figures S5E–S5H), phosphorylation of hPER2-S662 was significantly reduced by 60%–67% in three independent KO lines (Figures S5I and S5J).

Biochemical characterization of direct PER2 phosphorylation by MARK2 and MARK3

The experiments described above were performed with HEK cells. To investigate whether MARK2 and 3 directly phosphorylate hPER2 S662, we expressed recombinant forms of kinases in *E. coli*. hPER2 S662 but not PER2 S662A or S662D could be phosphorylated by the T208E form of MARK2, but not by the WT or the T208A mutant of MARK2 (Figures 3A and 3B). Similar results were obtained for MARK3 T211E (Figures S6A and S6B). MARK2 exhibited a significantly lower Km for the PER2 fragment (6.54 ± 2.06 μM) (Figure 3C) than MARK3 (23.04 ± 5.99 μM) (Figure S6C). This difference was later explained by our subsequent result that a specific binding between MARK2 and the PER2 498–556 region, which was absent in MARK3 (Figures 5A and 5D). Furthermore, Recombinant mouse MARK2 T208E (Figure 3D) and MARK3 T211E (Figure S6D) also phosphorylated mPER2 S659 but not S659A or S659D mutant. Together, these results have demonstrated that active forms of recombinant MARK2 and three directly phosphorylate PER2 at S662.

Our observations that MARK2 T208E mutant and MARK3 T211E mutant were active but their WT forms were not suggested that the WT forms required phosphorylation in mammalian cells, which was absent in *E. coli*. MARKs belong to the AMPK-Related Kinase (ARK) family, whose members could be activated by the kinase LKB1 or members of the STE20 family.[76,90] We therefore tested MAP4K7, a member of the STE20 subfamily of kinases. We used recombinant MAP4K7 to treat WT MARK2 or MARK3 purified from *E. coli*, they were indeed

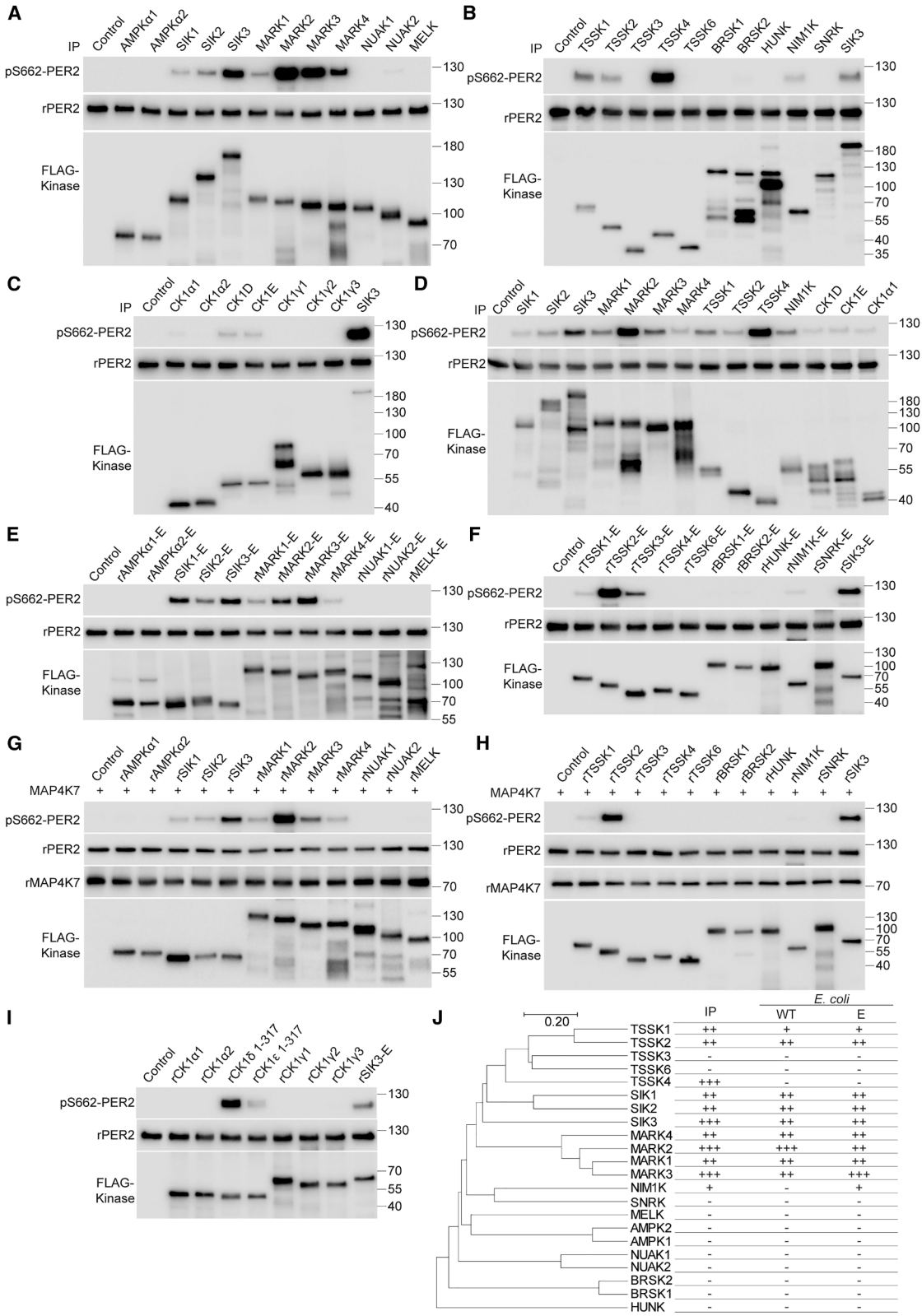

Figure 4. Phosphorylation of PER2 S662 by AMPK-related kinases (ARKs)

(A–D) Full-length forms of ARKs and CK1-related kinases tagged with the FLAG epitope were individually expressed in HEK293 cells and immunoprecipitated. Each was tested for activities on recombinant hPER2 556–771 (rPER2). SIK3 was used in all images as a reference of signal strength.

(legend continued on next page)

phosphorylated in the active loop (Figure 3E). Furthermore, MAP4K7 pretreated MARK2 and MARK3 could phosphorylate PER2-S662 (Figure 3E). Similarly, pretreatment with MAP4K7 also activated recombinant mouse MARK 2 or 3 purified from *E. coli*, making them able to phosphorylate mPER2-S659 (Figure 3F). These results demonstrate that MARKs are direct PER2 S662 kinases and that MARKs can be activated by upstream kinases such as those in the STE20 subfamily,[76,90] and suggest that it will be interesting to study regulation of MARKs *in vivo*.

In vitro phosphorylation of hPER2-S662 by ARKs

MARKs and TSSKs are members of the ARK family,[64–71] which we have recently characterized.[76,90] The salt-inducible kinases (SIK 1 and 3) are also ARK members, known to be regulators of circadian behavior: *Sik1* knockdown in the SCN resulted in a rapid phase shift of the circadian rhythm, resistance to jet lag,[91] while SIK3 promotes the destabilization of PER2, and its knockout lengthened the circadian period.[77]

We tested all ARKs for their activities on hPER2-S662 phosphorylation (Figure 4), with both ARKs immunoprecipitated from HEK cells (Figures 4A–4D and 4J) and ARKs purified from *E. coli* (Figures 4E–4H, 4J, and S7–S9). ARKs immunoprecipitated from HEK cells were full length WT proteins with the FLAG tag (Figures 4A–4D and 4J), while ARKs purified from *E. coli* were either full-length or truncated proteins containing the kinase domain, in either the WT form or with a phosphorylation-site mutation (T to E) in the activation loop (Figures 4E–4H, 4J, and S7). Recombinant WT ARKs from *E. coli* were pre-treated with MAP4K7 (Figures 4G and 4H) before being assayed for their kinase activities on hPER2 S662. SIK 1–3, MARK 1–4, TSSK1, 2 and 4, and NIM1K phosphorylated PER2-S662 (Figures 4A–4J), while MARK2, TSSK4 and MARK3 were the strongest. TSSK4 phosphorylated PER2-S662 only when immunoprecipitated from HEK cells, but not purified from *E. coli* (Figure 4J). Notablly, full-length CK1δ/ε had modest activities, whereas the truncated CK1δ/ε (1–317) variants were highly active after removal of their autoinhibitory C-terminal tails (Figures 4C and 4I).

PER2-S662 could not be phosphorylated by the following ARKs, whether they were immunoprecipitated from HEK cells or purified from *E. coli*: BRSK 1 or 2, AMPK 1 or 2, NUAK 1 or 2, MELK, SNRK, TSSK 3 or 6 (Figure 4J). PER2-S662 could be phosphorylated by TSSK4, only when it was immunoprecipitated from HEK cells but not from *E. coli* (Figure 4J).

MARK2 binding to, and stabilization of, PER2 in an S662-dependent manner

We examined potential interactions between MARKs and hPER2 using co-immunoprecipitation assays with an anti-FLAG antibody beads (Figure 5). MARK2, but not MARK3, specifically interacted with full-length PER2 (Figure 5A), which was confirmed reciprocally when FLAG-MARK2 and HA-PER2 were co-immunoprecipitated (Figure 5B).

To dissect domains in PER2 required for its interaction with MARK2, we separated hPER2 into four fragments (1–438, 321–557, 477–788 and 717–1,255). MARK2 interacted with full-length PER2, as well as fragments 321–557 and 477–788, but not PER2 (1–438) or PER2 (717–1,255). Further mapping of PER2 fragments showed that MARK2 interacted with PER2 498–557 (Figure 5D). This interaction domain is distinct from the S662 phosphorylation site, suggesting possible recruitment of MARK2 to PER2 to facilitate S662 phosphorylation.

Phosphorylation of PER2 S662 was known to increase its protein stability and the S662G mutation destabilized PER2.[41,43,46,48,51] To investigate whether MARK2 regulated PER2 stability, we transfected *Per2* (WT or S662G mutant) into HEK cells individually or co-transfected them with *Mark2*. We examined PER2 stability after cyclohexamide (CHX) blockade of protein translation. Co-transfection of *Mark2* increased the stability of PER2 (Figures 5E and 5F), indicating that MARK2 regulated PER2 stability. However, *Mark2* transfection did not affect the stability of the S662G mutant of PER2 (Figures 5G and 5H), indicating that MARK2 regulation of PER2 stability depends on S662 phosphorylation.

MARK2 regulation of cellular circadian rhythm in an S662-dependent manner

To investigate potential roles of MARKs in circadian regulation, we first over-expressed each of the four MARKs in D15 cells (*Per2::dLuc* U2OS cells). The circadian period was significantly lengthened if any of the four MARKs was over-expressed in D15 cells (Figure 6A for MARKs 2 and 3; Figures S10F–S10H for MARKs 1 and 4).

To investigate which *Mark(s)* was required for circadian regulation in D15 cells, we genetically targeted each of them and found no circadian phenotype in *Mark3* (Figure 6C) or *Mark1* (Figures S10I and S10K) KO cells. *Mark4* KO cells showed modest but significant period shortening (Figures S10J and S10K). *Mark2* KO cells exhibited significantly shortened period by ~1.13 h (Figure 6C).

To determine whether MARK2 regulates circadian period in an S662-dependent manner, we introduced *Per2 S662G* mutation into D15 cells (Figure S10L). The *S662G* mutant cells displayed a significantly shortened circadian period compared to WT cells (Figure 6E). Furthermore, while *Mark2* KO shortened the period in WT cells (Figure 6C), it failed to do so in *Per2 S662G* mutant cells (Figure 6G),indicating that MARK2 regulates circadian period in an S662-dependent manner.

(E–H) FLAG tagged full-length or fragments of ARKs and CK1-related kinases were individually purified from *E. coli* before being assayed with recombinant PER2 556–771. (E and F), In case where the WT forms of ARKs could not phosphorylate rPER2, recombinant ARKs with T to E mutants in their activation loops (Figure S7) were purified from *E. coli* before being tested for their activities on rPER2. Recombinant WT forms of ARKs purified from *E. coli* were pre-incubated with MAP4K7 for 1 h before being tested for their activities on recombinant hPER2.

(I) FLAG-tagged CK1-related kinases were individually purified from *E. coli* and assayed with rPER2. Recombinant CK1δ and CK1ε were N-terminal truncated proteins with kinase domain (residue 1–317), while other CK1 family members were full-length proteins.

(J) Summary of PER2 S662 phosphorylation by ARKs in the phylogeny tree. The "IP" column represents the abilities of the 22 kinases immunoprecipitated from HEK293 to phosphorylate PER2 S662. The "WT" and "E" columns represent the abilities of the 22 WT kinases expressed in *E. coli* and their mutant forms with the activation loop phosphorylation T site mutated to E, respectively. See also Figures S7–S9.

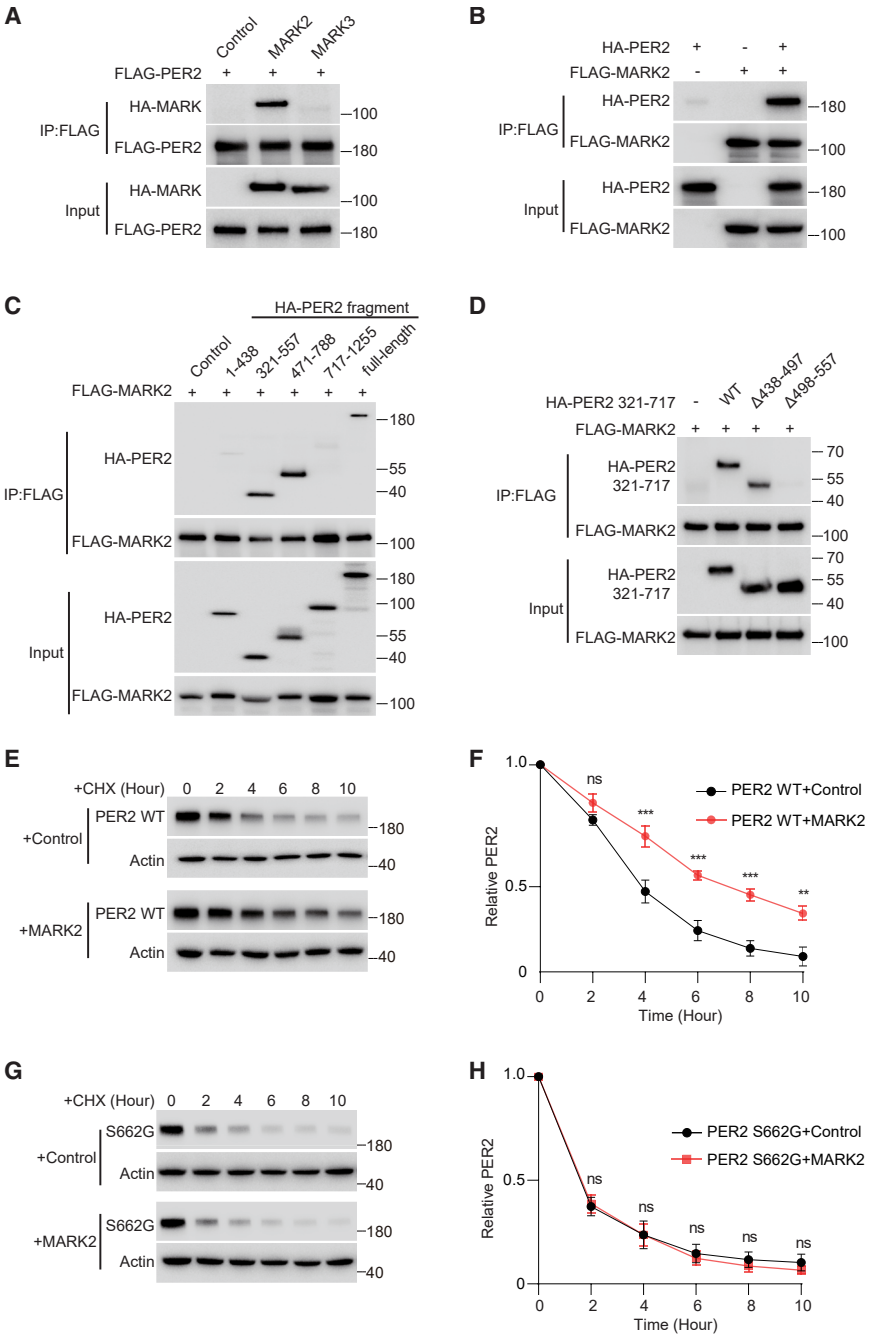

Figure 5. MARK2 interaction with and stabilization of PER2 protein

(A and B) MARK2 interacted with PER2. HEK293 cells were co-transfected with FLAG-tagged *MARK2* and HA-tagged full-length *PER2*. Co-Immunoprecipitation (Co-IP) was performed by anti-FLAG beads (A). Reciprocally Co-IP was also performed using FLAG-*MARK2* and HA-*PER2* (B).

(C and D) MARK2 interacted with PER2 498–557. HEK293 cells were co-transfected with FLAG-tagged *MARK2* and HA-tagged *PER2* truncated fragments, as well as the full-length *PER2*. Co-IP was performed by anti-FLAG beads. Deletion of 498–557 from PER2 321–717 eliminated PER2 interaction with MARK2.

(E–H) MARK2 attenuated PER2 degradation in an S662 phosphorylation-dependent manner. HEK293 cells were transfected with *PER2 WT* (E) or *S662G* mutant (G) individually or co-transfected with *MARK2* for 24 h. Transfected cells were treated with 200 mM cycloheximide (CHX) before being harvested at indicated time points. Western blots were quantified by the ImageJ software (n = 3 independent biological replicates), and data were analyzed by the GraphPad software (F and H). The degradation of PER2 WT was slowed down by *MARK2* co-expression (E and F). PER2 S662G degradation was faster than WT PER2 and its degradation rate was not affected when co-expressed with MARK2 (G and H). Two-way ANOVA by Sidak's multiple comparisons (F and H), data are presented as mean ± SEM.

Consistent with these, biochemical analyses showed that over-expression of MARK2 or MARK3 enhanced PER2 S662 phosphorylation and increased PER2 protein stability (Figure 6B), whereas *Mark2* KO reduced both (Figure 6D). The *PER2 S662G* mutant cells showed lower basal PER2 levels than WT cells (Figure 6F). Importantly, while *Mark2* KO reduced PER2 protein level in *PER2 WT* cells (Figure 6D), this effect was completely abolished in *PER2 S662G* mutant cells (Figure 6H). Together, these results demonstrate that MARK2 acts upstream of PER2 S662, regulating PER2 stability and circadian period length in an S662-dependent manner.

Physiological significance of *Mark2* but not *Mark3* in regulating the circadian rhythm

To investigate physiological roles of MARK kinases in circadian regulation, we generated *Mark2* and *Mark3* mutants in mice (Figure S11). Because *Mark2* KO mice were embryonic lethal, we generated mice with conditional *Mark2* KO (*Mark2*$^{flox/flox}$) (Figure S11A) and crossed them with Nestin-Cre mice to delete neuronal *Mark2* in the central nervous system (CNS). Mice were entrained to a 12-h light/12-h dark (LD) cycle for 14 days, followed by 21 days of constant darkness (DD),with locomotion continuously recorded by the running wheel system (Figure 7).

The circadian rhythm of *Nestin-Cre*; *Mark2*$^{flox/flox}$ mice was significantly different from that of control mice (*Nestin-Cre*; *Mark2*$^{+/+}$): with advanced onset (*Nestin-Cre*; *Mark2*$^{flox/flox}$: ZT 12.05 ± 0.09 versus *Nestin-Cre*; *Mark2*$^{+/+}$: ZT 12.37 ± 0.09, Figures 7A and 7C) and shortened period length (~0.2 h, *Nestin-Cre*; *Mark2*$^{flox/flox}$: 23.76 ± 0.02 versus *Nestin-Cre*; *Mark2*$^{+/+}$: 23.96 ± 0.03, Figures 7A and 7D). Although both *Nestin-Cre*; *Mark2*$^{flox/+}$ and *Nestin-Cre*; *Mark2*$^{flox/flox}$ mice exhibited comparable reductions in locomotor activities (Figure 7B), advanced phase and shortened period were only observed in

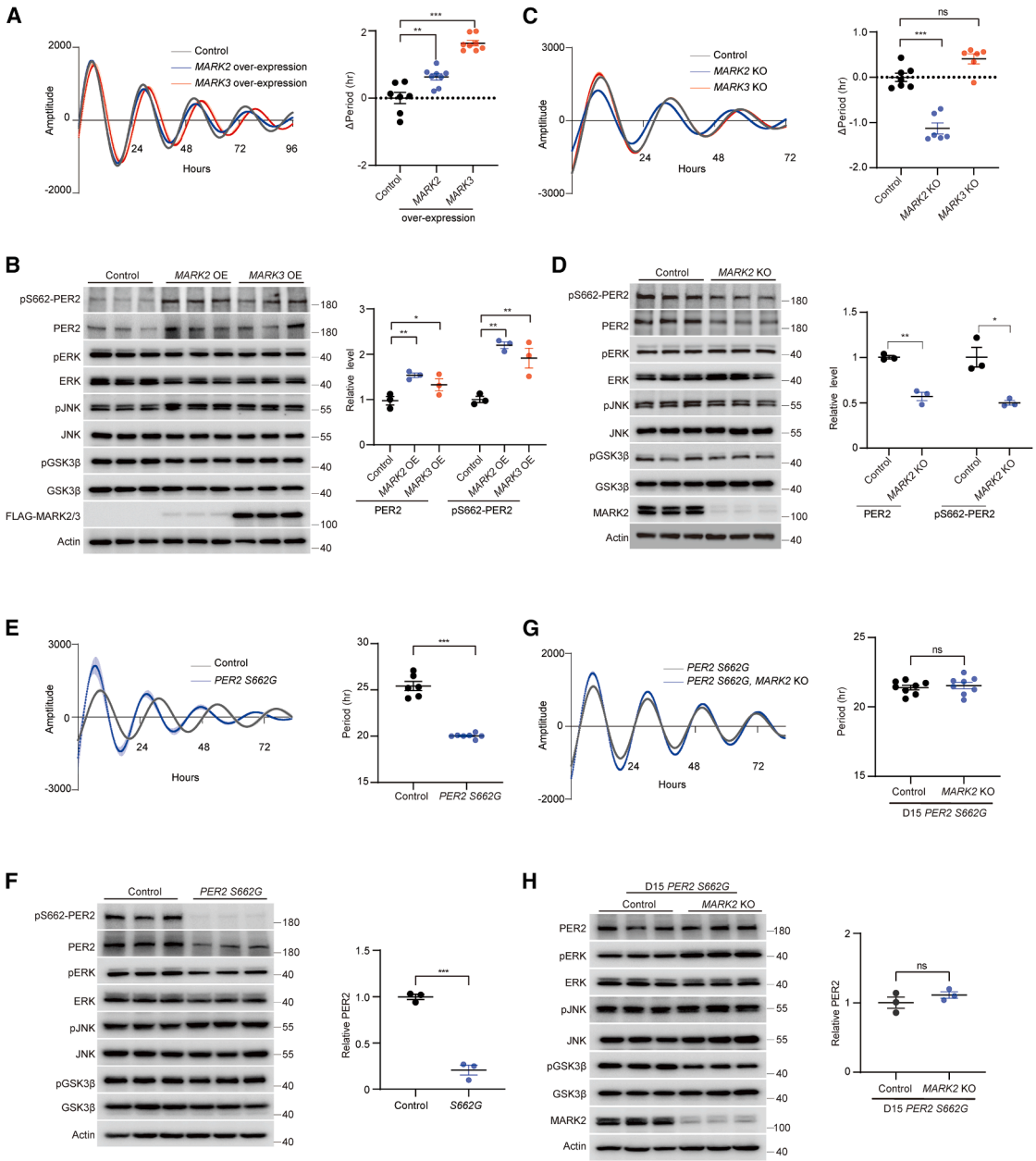

Figure 6. *MARK2* regulation of the circadian period via PER2 S662 in a human cell line

(A) Over-expression (OE) of MARK 2 or 3 prolonged the rhythm of D15 cells by 0.63 or 1.63 h, respectively. Stable MARK2 or MARK3 over-expression D15 cells were individually generated using a lentiviral system. Representative oscillatory data and rhythm changes were shown (control, $n = 7$; *MARK2*, $n = 8$; *MARK3*, $n = 8$ independent biological replicates).

(B) MARK2 or MARK3 over-expression increased PER2-S662 phosphorylation and total PER2 protein levels. Neither MARK2 nor MARK3 over-expression changed the phosphorylation or the total levels of ERK, JNK or GSK3β. Western blots were quantified by the ImageJ ($n = 3$ independent biological replicates).

(C) KO of *MARK2* but not *MARK3* shortened the circadian period of D15 cells (control, $n = 7$; *MARK2* KO: $n = 6$; *MARK3* KO: $n = 6$ independent biological replicates).

(D) *MARK2* KO reduced both phosphorylation of PER2 S662 and total PER2 protein levels, without affecting ERK, JNK or GSK3β. Western blots were quantified by the ImageJ ($n = 3$ independent biological replicates).

(E and F) The *PER2 S662G* mutation shortened circadian period to 20.01 h (control, $n = 6$; *S662G*: $n = 7$ independent biological replicates) and reduced PER2 protein abundance in D15 cells. *PER2 S662G* mutation was introduced into D15 cells confirmed by PCR and sequencing (Figure S10L). Western blots were quantified by the ImageJ ($n = 3$ independent replicates).

(G and H) *MARK2* KO failed to shorten the circadian period (*S662G*: $n = 8$; *S662G & MARK2* KO: $n = 8$ independent replicates) or reduce PER2 abundance ($n = 3$ independent replicates) in *S662G* mutant cells. Western blots were quantified by the ImageJ ($n = 3$ independent replicates). One ANOVA followed by Dunnett's multiple comparisons test (A–D); unpaired Student's *t* test (E–H). Data are presented as mean ± SEM. See also Figure S10 and Table S3.

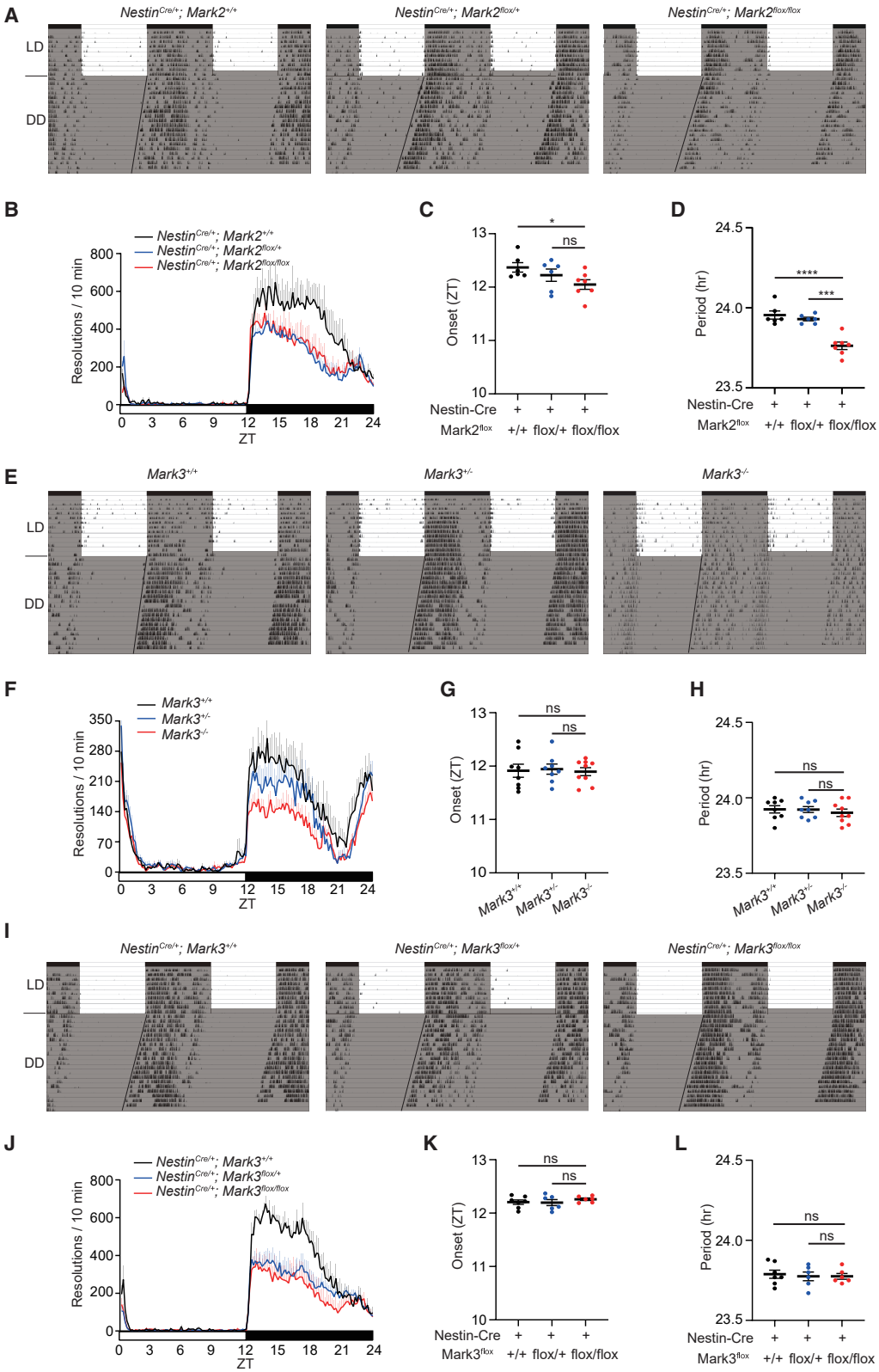

Figure 7. Requirement of neuronal *Mark2*, but not *Mark3*, in physiological regulation of the circadian rhythm

(A–D) Wheel-running analysis of circadian rhythms of $Nestin^{Cre/+}$; $Mark2^{+/+}$ (n = 6), $Nestin^{Cre/+}$; $Mark2^{+/flox}$ (n = 6), $Nestin^{Cre/+}$; $Mark2^{flox/flox}$ (n = 7) mice. Gray shading indicates nighttime (light off). Representative plots of running-wheel activities (A), daily wheel revolutions per 10 min in LD (B), activity onsets in LD (C), and period length in DD (D).

(legend continued on next page)

Nestin-Cre; *Mark2*$^{flox/flox}$ mice, supporting that the circadian phenotype in *Nestin-Cre*; *Mark2*$^{flox/flox}$ mice was independent of locomotor activities (Figure 7C). Thus, phase-advanced and shortened period phenotypes in *Nestin-Cre*; *Mark2*$^{flox/flox}$ mice were confirmed.

Neither conventional nor neuronal specific *Mark3* knockout mice (Figure S11B) showed significant alterations in activity onset (Figures 7G and 7K) or circadian period (Figures 7H and 7L), despite a reduction in locomotor activities (Figures 7F and 7J). These results are consistent with cellular findings in human D15 cells and indicate that *Mark3* is not involved in circadian regulation.

Because *Mark4* KO showed a modest but significant period shortening in D15 cells (Figures S10J and S10K), we generated *Mark4* conditional knockout mice (Figure S11C). We found that these mice exhibited normal circadian rhythm (Figures S11D–S11G).

In summary, results from genetically targeted mice reveal that only mutants for *Mark2* but not *Mark3* or *Mark4* showed phenotype similar to the human FASPS,[43,61] demonstrating that *Mark2* is essential for circadian regulation *in vivo*.

DISCUSSION

After 24 years from the initial finding of of the *PER2 S662G* mutation in humans with the FASP syndrome,[48] we have identified MARK2 as a kinase that is not only able to biochemically phosphorylate PER2 S662 *in vitro*, but is also physiologically required for regulating the circadian rhythm *in vivo* in an S662-dependent manner. In our efforts to find the upstream kinases for PER2 S662, we have found seven kinases which could biochemically phosphorylate PER2 at S662, but their individual loss of function mutations in mice did not show the circadian phase advancement phenotype consistent with the *S662G* mutation in humans. While we cannot rule out the possibility of more than one kinase regulating PER2 S662 endogenously, our approach has shown the effectiveness of biochemical purification in solving a physiological puzzle.

Phosphorylation of PER2 S662 by multiple kinases *in vitro*

Since the discovery of *hPER2 S662G* mutation in FASPS,[43,61] there has been much interest in finding the kinase(s) capable of phosphorylating S662. Early work by others[41,43,46,51,57–59,88,92] and ourselves have found that CK1δ and CK1ε act as key kinases phosphorylate S662. However, dual knockout of *CK1δ* and *CK1ε* in HEK293 cells markedly reduced, but did not abolish S662 phosphorylation. This prompted a biochemical purification approach, which led to the discovery of microtubule affinity-regulating kinases 2 and 3 (MARK2 and MARK3) as robust S662 kinases. They belong to the subfamily of adenosine monophosphate (AMP)-activated protein kinase (AMPK) related kinases (ARKs).[64–76] A subsequent comparison of the *in vitro* activities of all ARK members against PER2-S662 is summarized in Figure 4J, we have found that, *in vitro*, multiple members of the ARKs could phosphorylate S662 of hPER2. These include SIK 1, 2, and 3, MARK 1, 2, 3, and 4, TSSK 1 and 2. S662 was not phosphorylated *in vitro* by TSSK6, SNRK, MELK, AMPK 1 or 2, NUAK 1 or 2, BRSK 1 or 2, or HUNK (Figure 4). However, SIK3 knockdown in mice lengthened the period,[77] while KO of SIK 1 or 2 published previously by us,[78,79] and single or double KO of TSSK 1 or 2 shown by us here (Figure S4) did not reveal significant circadian changes. All these apparent failures suggest that there are multiple kinases for S662, which may function redundantly for S662 phosphorylation or have opposing effects on other clock components *in vivo*.

Functional significance of *MARK2 in vivo*

Among the four *MARK* family members, over-expression of any of them could lead to longer period in human D15 cells (Figures 6 and S10). KO of *MARK 2* or *4* shortened period in D15 cells (Figures 6 and S10), whereas KO of neither *MARK 1* nor *3* showed any circadian phenotype in D15 cells.

The biochemical and circadian phenotypes of *MARK2* KO were eliminated in *PER2 S662G* mutant D15 cells (Figures 6G and 6H). These results not only support a role for *MARK2* in circadian regulation but also indicate that MARK2 functions upstream of hPER2 S662.

The most important result showing physiological significance of *MARK2* came from *in vivo* studies with mouse mutants. Neuronal specific KO of *Mark2* showed both advanced onset and shortened period length (~0.2 h, Figures 7A–7D), whereas conventional and neuronal specific *Mark3* KO mice and neuronal specific *Mark4* KO mice exhibited no circadian phenotype. Thus, we have finally discovered *Mark2* as a physiologically relevant kinase that regulates the circadian rhythm in an S662-dependent manner.

We can not rule out the possibility that multiple kinases, including those discovered by us here, may function redundantly with MARK2 in regulating PER2-S662 phosphorylation and circadian rhythm. It is possible that several kinases may regulate more than one site in PER2 and more sites in additional proteins involved in circadian regulation.

MARK2, PER2 phosphorylation and stability

Posttranslational modifications, especially phosphorylation, are important in clock regulation (Crane et al., 2014; Gallego et al., 2007; Mehra et al., 2009; Reischl et al., 2011). In *Drosophila* and mammals, PER proteins are phosphorylated and defective PER phosphorylation causes circadian disruption.[36,40,41,43,46,48,50,51,52,56–60,62,88,93–121]

Phosphorylation of different sites and different proteins regulate circadian rhythm differently. In the case of S662, its phosphorylation stabilizes PER2 protein,[41,43,46] which we have confirmed here (Figures 5E and 5F). Furthermore, MARK2 increased PER2 stability, an effect shown to be dependent on

(E–H) Representative plots of running-wheel activities of *Mark3*$^{+/+}$ (n = 8), *Mark3*$^{+/-}$ (n = 8), and *Mark3*$^{-/-}$ mice (n = 9). *Mark3* KO mice showed no significant changes in activity onset (G) or period (H), despite reduced activity (F).

(I–L) Wheel-running analysis of circadian rhythms of *Nestin*$^{Cre/+}$; *Mark3*$^{+/+}$ (n = 7), *Nestin*$^{Cre/+}$; *Mark3*$^{+/flox}$ (n = 6), *Nestin*$^{Cre/+}$; *Mark3*$^{flox/flox}$ (n = 6) mice. Neuronal-specific *Mark3* KO mice showed no significant circadian phenotype. One-way ANOVA followed by Tukey's multiple comparisons test (C, D, G, H, K, and L); data are presented as mean ± SEM. See also Figure S11 and Table S4.

S662 because S662G PER2 could not be stabilized by MARK2 (Figures 5G and 5H).

High-fat diet enhances PER2 phosphorylation at S662, whereas fasting reduces it and causes a phase advance in behavioral rhythms.[122] Given that MARKs and other ARKs are activated by the upstream kinase LKB1,[123–126] whose activity is modulated by diverse stimuli: promoted by high osmolarity and amyloid precursor protein (APP) accumulation, suppressed by short-term fasting.[127,128] It will be interesting to investigate whether the LKB1-ARK signaling axis serves as an integrator, translating metabolic information into circadian timing by regulating PER2 S662 phosphorylation.

The biochemical approach to understanding molecular basis of circadian regulation

The genetic approach is powerful in molecular studies of the circadian rhythm. It became a standard since the discoveries of genetic mutants in *Drosophila*,[13] *Neurospora,*[14] and *Chlamydomonas*.[15] The genetical approach requires whole animals to discover genes involved in circadian regulation, which is relatively easy in simple animals but more difficult in mammals.

The biochemical approach is more powerful in identifying biochemical regulators of proteins known to be involved in circadian regulation, but the *in vitro* biochemical activities may or may not correlate with functional significance *in vivo*. The biochemical approach is often, though not always, closer than the genetic approach in reaching a mechanistic understanding. In the present case, MARK2 is upstream of PER2 by phosphorylating its S662 and stabilizing the PER2 protein.

In summary, we have taken a biochemical approach of protein purification to discover kinases capable of phosphorylation S662 of hPER2 and among those discovered, we have found that *Mark2* in the mouse brain is physiologically significant in regulating the circadian rhythm.

Limitations of the study

Our biochemical purification approach, while effective, was conducted using HEK293 cell lysates, which may not fully represent the endogenous kinases in the SCN, the master clock. Our Nestin-Cre-driven knockout removed *Mark2* in neurons, whereas the SCN consists of heterogeneous cell populations (e.g., AVP-, VIP-, GRP-, or CCK-expressing neurons, and glia). Cell type-specific deletion within these subpopulations is required to better define the function of MARK2. Additionally, although CK1δ/ε is an established kinase for PER2 S662, it remains unclear how MARK2 activity is regulated by upstream signaling and whether it cooperates with CK1δ/ε to regulate the clock. We identified several other kinases (SIK1-3, TSSK1/2/4, NIM1K) that phosphorylated PER2 S662 *in vitro*. Their physiological roles and functional contexts *in vivo* remain to be studied.

RESOURCE AVAILABILITY

Lead contact

Further information and requests for resources and reagents should be directed to and will be fulfilled by the lead contact, Yi Rao (yrao@pku.edu.cn).

Materials availability

All unique/stable reagents generated in this study are available from the lead contact without restriction.

Data and code availability

- Data reported in this article will be shared by the lead contact upon request.
- This article does not report original code.
- Any additional information required to reanalyze the data reported in this article is available from the lead contact upon request.

ACKNOWLEDGMENTS

We are grateful to Drs. Dong Liu and Qi Zhang at the National Center for Protein Sciences of Peking University for help with MS sample preparing and data analysis, the National Center for Protein Sciences at Peking University for access to instrumentation. Research in the Rao laboratory has never been contaminated by the Chinese Brain Initiative.

AUTHOR CONTRIBUTIONS

Y.R. supervised the project, Y.R., Y. Liu, Y. Li, T.V.W., and T.Y. designed the experiments. Y.R., Y. Liu, Y. Li, and T.V.W. wrote the manuscript, with input from all co-authors. Y. Liu performed biochemical purifications and *in vitro* assays, Y. Li performed circadian experiments on mice, T.V.W. performed experiments with D15 cells, T.Y. performed the experiments on cDNA screen with phos-tag. J.H. generated the genetic mutant mice.

DECLARATION OF INTERESTS

The authors declare no competing interests.

STAR★METHODS

Detailed methods are provided in the online version of this paper and include the following:

- KEY RESOURCES TABLE
- EXPERIMENTAL MODEL AND STUDY PARTICIPANT DETAILS
  - Cell lines
  - Animals
- METHOD DETAILS
  - Detection of phosphorylation by phos-tag
  - Expression and purification of recombinant proteins
  - Purification of MARK 2 and 3 from HEK293T cells
  - *In vitro* kinase assay
  - Calculation of the Michaelis-Menten constant
  - Protein stability assay
  - Generation of KO cell lines
  - Circadian rhythm analysis of D15 cells
  - Generation of PER2 S662G mutant D15 cells with prime editing 7
  - Mouse stocks
  - Wheel running assays of circadian rhythms in mice
- QUANTIFICATION AND STATISTICAL ANALYSIS

SUPPLEMENTAL INFORMATION

Supplemental information can be found online at https://doi.org/10.1016/j.chembiol.2026.02.007.

Received: July 24, 2025
Revised: November 18, 2025
Accepted: February 17, 2026
Published: March 10, 2026

REFERENCES

1. Roenneberg, T., and Merrow, M. (2016). The Circadian Clock and Human Health. Curr. Biol. *26*, R432–R443.
2. Parsons, M.J., Moffitt, T.E., Gregory, A.M., Goldman-Mellor, S., Nolan, P.M., Poulton, R., and Caspi, A. (2015). Social jetlag, obesity

and metabolic disorder: investigation in a cohort study. Int. J. Obes. *39*, 842–848.

3. Ohlander, J., Keskin, M.C., Stork, J., and Radon, K. (2015). Shift work and hypertension: Prevalence and analysis of disease pathways in a German car manufacturing company. Am. J. Ind. Med. *58*, 549–560.
4. Roenneberg, T., Allebrandt, K.V., Merrow, M., and Vetter, C. (2012). Social jetlag and obesity. Curr. Biol. *22*, 939–943.
5. Schernhammer, E.S., Laden, F., Speizer, F.E., Willett, W.C., Hunter, D.J., Kawachi, I., Fuchs, C.S., and Colditz, G.A. (2003). Night-shift work and risk of colorectal cancer in the nurses' health study. J. Natl. Cancer Inst. *95*, 825–828.
6. Tynes, T., Hannevik, M., Andersen, A., Vistnes, A.I., and Haldorsen, T. (1996). Incidence of breast cancer in Norwegian female radio and telegraph operators. Cancer Causes Control. *7*, 197–204.
7. Azmi, N.A.S.M., Juliana, N., Teng, N.I.M.F., Azmani, S., Das, S., and Effendy, N. (2020). Consequences of Circadian Disruption in Shift Workers on Chrononutrition and their Psychosocial Well-Being. Int. J. Environ. Res. Publ. Health *17*, 2043.
8. Curtis, A.M., Bellet, M.M., Sassone-Corsi, P., and O'Neill, L.A.J. (2014). Circadian Clock Proteins and Immunity. Immunity *40*, 178–186.
9. Chong, S.Y.C., Ptáček, L.J., and Fu, Y.H. (2012). Genetic insights on sleep schedules: this time, it's PERsonal. Trends Genet. *28*, 598–605.
10. Bass, J., and Takahashi, J.S. (2010). Circadian Integration of Metabolism and Energetics. Science *330*, 1349–1354.
11. Mohawk, J.A., and Takahashi, J.S. (2011). Cell autonomy and synchrony of suprachiasmatic nucleus circadian oscillators. Trends Neurosci. *34*, 349–358.
12. Dibner, C., Schibler, U., and Albrecht, U. (2010). The mammalian circadian timing system: organization and coordination of central and peripheral clocks. Annu. Rev. Physiol. *72*, 517–549.
13. Konopka, R.J., and Benzer, S. (1971). Clock mutants of Drosophila melanogaster. Proc. Natl. Acad. Sci. USA *68*, 2112–2116.
14. Feldman, J.F., and Menaker, M. (1971). Waser In: New mutations affecting circadian rhythmicity in *Neurospora*. In Biochronometry. (National Academy of Sciences), pp. 652–656.
15. Bruce, V.G. (1972). Mutants of the biological clock in Chlamydomonas reinhardi. Genetics *70*, 537–548.
16. Lowrey, P.L., and Takahashi, J.S. (2011). Genetics of Circadian Rhythms in Mammalian Model Organisms. Adv. Genet. *74*, 175–230.
17. Crane, B.R., and Young, M.W. (2014). Interactive features of proteins composing eukaryotic circadian clocks. Annu. Rev. Biochem. *83*, 191–219.
18. Panda, S., Hogenesch, J.B., and Kay, S.A. (2002). Circadian rhythms from flies to human. Nature *417*, 329–335.
19. Reppert, S.M., and Weaver, D.R. (2001). Molecular analysis of mammalian circadian rhythms. Annu. Rev. Physiol. *63*, 647–676.
20. Allada, R., Emery, P., Takahashi, J.S., and Rosbash, M. (2001). Stopping time: the genetics of fly and mouse circadian clocks. Annu. Rev. Neurosci. *24*, 1091–1119.
21. Hardin, P.E., Hall, J.C., and Rosbash, M. (1990). Feedback of the Drosophila period gene product on circadian cycling of its messenger RNA levels. Nature *343*, 536–540.
22. Zheng, X., and Sehgal, A. (2012). Speed control: cogs and gears that drive the circadian clock. Trends Neurosci. *35*, 574–585.
23. Nitabach, M.N., and Taghert, P.H. (2008). Organization of the Drosophila circadian control circuit. Curr. Biol. *18*, R84–R93.
24. Vitaterna, M.H., Shimomura, K., and Jiang, P. (2019). Genetics of Circadian Rhythms. Neurol. Clin. *37*, 487–504.
25. Shearman, L.P., Sriram, S., Weaver, D.R., Maywood, E.S., Chaves, I., Zheng, B., Kume, K., Lee, C.C., van der Horst, G.T., Hastings, M.H., and Reppert, S.M. (2000). Interacting molecular loops in the mammalian circadian clock. Science *288*, 1013–1019.
26. Zheng, B., Larkin, D.W., Albrecht, U., Sun, Z.S., Sage, M., Eichele, G., Lee, C.C., and Bradley, A. (1999). The mPer2 gene encodes a functional component of the mammalian circadian clock. Nature *400*, 169–173.
27. Kume, K., Zylka, M.J., Sriram, S., Shearman, L.P., Weaver, D.R., Jin, X., Maywood, E.S., Hastings, M.H., and Reppert, S.M. (1999). mCRY1 and mCRY2 are essential components of the negative limb of the circadian clock feedback loop. Cell *98*, 193–205.
28. Hogenesch, J.B., Gu, Y.Z., Jain, S., and Bradfield, C.A. (1998). The basic-helix-loop-helix-PAS orphan MOP3 forms transcriptionally active complexes with circadian and hypoxia factors. Proc. Natl. Acad. Sci. USA *95*, 5474–5479.
29. Gekakis, N., Staknis, D., Nguyen, H.B., Davis, F.C., Wilsbacher, L.D., King, D.P., Takahashi, J.S., and Weitz, C.J. (1998). Role of the CLOCK protein in the mammalian circadian mechanism. Science *280*, 1564–1569.
30. Shearman, L.P., Zylka, M.J., Weaver, D.R., Kolakowski, L.F., Jr., and Reppert, S.M. (1997). Two period homologs: circadian expression and photic regulation in the suprachiasmatic nuclei. Neuron *19*, 1261–1269.
31. Chen, R., Schirmer, A., Lee, Y., Lee, H., Kumar, V., Yoo, S.H., Takahashi, J.S., and Lee, C. (2009). Rhythmic PER Abundance Defines a Critical Nodal Point for Negative Feedback within the Circadian Clock Mechanism. Mol. Cell *36*, 417–430.
32. Lee, H., Chen, R., Lee, Y., Yoo, S., and Lee, C. (2009). Essential roles of CKIδ and CKIε in the mammalian circadian clock. Proc. Natl. Acad. Sci. USA *106*, 21359–21364.
33. Cao, X., Yang, Y., Selby, C.P., Liu, Z., and Sancar, A. (2021). Molecular mechanism of the repressive phase of the mammalian circadian clock. Proc. Natl. Acad. Sci. USA *118*, e2021174118.
34. Aryal, R.P., Kwak, P.B., Tamayo, A.G., Gebert, M., Chiu, P.L., Walz, T., and Weitz, C.J. (2017). Macromolecular Assemblies of the Mammalian Circadian Clock. Mol. Cell *67*, 770–782.e6.
35. Park, J., Lee, K.J., Kim, H., Shin, H., and Lee, C.G. (2023). Endogenous circadian reporters reveal functional differences of paralogs and the significance of PERIOD:CK 1 stable interaction. Proc. Natl. Acad. Sci. USA *120*, e2212255120.
36. An, Y., Yuan, B., Xie, P., Gu, Y., Liu, Z., Wang, T., Li, Z., Xu, Y., and Liu, Y. (2022). Decoupling PER phosphorylation, stability and rhythmic expression from circadian clock function by abolishing PER-CK1 interaction. Nat. Commun. *13*, 3991.
37. Preitner, N., Damiola, F., Lopez-Molina, L., Zakany, J., Duboule, D., Albrecht, U., and Schibler, U. (2002). The orphan nuclear receptor REV-ERBalpha controls circadian transcription within the positive limb of the mammalian circadian oscillator. Cell *110*, 251–260.
38. Liao, M., Liu, Y., Xu, Z., Fang, M., Yu, Z., Cui, Y., Sun, Z., Huo, R., Yang, J., Huang, F., et al. (2025). The P-loop NTPase RUVBL2 is a conserved clock component across eukaryotes. Nature *10*, 1038.
39. Lee, C., Etchegaray, J.P., Cagampang, F.R., Loudon, A.S., and Reppert, S.M. (2001). Posttranslational mechanisms regulate the mammalian circadian clock. Cell *107*, 855–867.
40. Chen, R., Schirmer, A., Lee, Y., Lee, H., Kumar, V., Yoo, S.H., Takahashi, J.S., and Lee, C. (2009). Rhythmic PER abundance defines a critical nodal point for negative feedback within the circadian clock mechanism. Mol. Cell *36*, 417–430.
41. Vanselow, K., Vanselow, J.T., Westermark, P.O., Reischl, S., Maier, B., Korte, T., Herrmann, A., Herzel, H., Schlosser, A., and Kramer, A. (2006). Differential effects of PER2 phosphorylation: molecular basis for the human familial advanced sleep phase syndrome (FASPS). Gene Dev. *20*, 2660–2672.
42. Fu, Y., Jones, C.R., Toh, K., Virshup, D., and Ptacek, L.J. (2001). An hPer2 phosphorylation site mutation in familial Advanced Sleep-Phase Syndrome. Am. J. Hum. Genet. *69*, 597.

43. Xu, Y., Toh, K.L., Jones, C.R., Shin, J.Y., Fu, Y.H., and Ptácek, L.J. (2007). Modeling of a human circadian mutation yields insights into clock regulation by PER2. Cell *128*, 59–70.

44. Ohsaki, K., Oishi, K., Kozono, Y., Nakayama, K., Nakayama, K.I., and Ishida, N. (2008). The Role of β-TrCP1 and β-TrCP2 in Circadian Rhythm Generation by Mediating Degradation of Clock Protein PER2. J. Biochem. *144*, 609–618.

45. Cao, X., Wang, L., Selby, C.P., Lindsey-Boltz, L.A., and Sancar, A. (2023). Analysis of mammalian circadian clock protein complexes over a circadian cycle. J. Biol. Chem. *299*, 102929.

46. Xu, Y., Padiath, Q.S., Shapiro, R.E., Jones, C.R., Wu, S.C., Saigoh, N., Saigoh, K., Ptácek, L.J., and Fu, Y.H. (2005). Functional consequences of a CKI δ mutation causing familial advanced sleep phase syndrome. Nature *434*, 640–644.

47. Flotow, H., Graves, P.R., Wang, A.Q., Fiol, C.J., Roeske, R.W., and Roach, P.J. (1990). Phosphate groups as substrate determinants for casein kinase I action. J. Biol. Chem. *265*, 14264–14269.

48. Toh, K.L., Jones, C.R., He, Y., Eide, E.J., Hinz, W.A., Virshup, D.M., Ptácek, L.J., and Fu, Y.H. (2001). An hPer2 phosphorylation site mutation in familial advanced sleep phase syndrome. Science *291*, 1040–1043.

49. Gallego, M., and Virshup, D.M. (2007). Post-translational modifications regulate the ticking of the circadian clock. Nat. Rev. Mol. Cell Biol. *8*, 139–148.

50. Zhou, M., Kim, J.K., Eng, G.W.L., Forger, D.B., and Virshup, D.M. (2015). A Period2 phosphoswitch regulates and temperature compensates circadian period. Mol. Cell *60*, 77–88.

51. Narasimamurthy, R., Hunt, S.R., Lu, Y., Fustin, J.M., Okamura, H., Partch, C.L., Forger, D.B., Kim, J.K., and Virshup, D.M. (2018). CK1δ/ε protein kinase primes the PER2 circadian phosphoswitch. Proc. Natl. Acad. Sci. USA *115*, 5986–5991.

52. Masuda, S., Narasimamurthy, R., Yoshitane, H., Kim, J.K., Fukada, Y., and Virshup, D.M. (2020). Mutation of a PER2 phosphodegron perturbs the circadian phosphoswitch. Proc. Natl. Acad. Sci. USA *117*, 10888–10896.

53. Cullati, S., Akizuki, K., Chen, J.S., Johnson, J., Yaron, T., Cantley, L., and Gould, K. (2024). Substrate displacement of CK1 C-termini regulates kinase specificity. J. Biol. Chem. *300*, S706.

54. Francisco, J.C., and Virshup, D.M. (2024). Hierarchical and scaffolded phosphorylation of two degrons controls PER2 stability. J. Biol. Chem. *300*, 107391.

55. Francisco, J.C., and Virshup, D.M. (2022). Casein Kinase 1 and Human Disease: Insights From the Circadian Phosphoswitch. Front. Mol. Biosci. *9*, 911764.

56. Ricci, C.G., Philpott, J.M., Torgrimson, M.R., Freeberg, A.M., Narasimamurthy, R., de Barros, E.P., Amaro, R., Virshup, D.M., McCammon, J.A., and Partch, C.L. (2025). Markovian state models uncover casein kinase 1 dynamics that govern circadian period. Biophys. J. *124*, 4034–4048.

57. Philpott, J.M., Freeberg, A.M., Park, J., Lee, K., Ricci, C.G., Hunt, S.R., Narasimamurthy, R., Segal, D.H., Robles, R., Cai, Y., et al. (2023). PERIOD phosphorylation leads to feedback inhibition of CK1 activity to control circadian period. Mol. Cell *83*, 1677–1692.e8.

58. Philpott, J.M., Narasimamurthy, R., Ricci, C.G., Freeberg, A.M., Hunt, S.R., Yee, L.E., Pelofsky, R.S., Tripathi, S., Virshup, D.M., and Partch, C.L. (2020). Casein kinase 1 dynamics underlie substrate selectivity and the PER2 circadian phosphoswitch. eLife *9*, e52343.

59. Philpott, J.M., Torgrimson, M.R., Harold, R.L., and Partch, C.L. (2022). Biochemical mechanisms of period control within the mammalian circadian clock. Semin. Cell Dev. Biol. *126*, 71–78.

60. Shanware, N.P., Hutchinson, J.A., Kim, S.H., Zhan, L., Bowler, M.J., and Tibbetts, R.S. (2011). Casein kinase 1-dependent phosphorylation of familial advanced sleep phase syndrome-associated residues controls PERIOD 2 stability. J. Biol. Chem. *286*, 12766–12774.

61. Toh, K.L., Jones, C.R., He, Y., Eide, E.J., Hinz, W.A., Virshup, D.M., Ptácek, L.J., and Fu, Y.H. (2001). An hPer2 phosphorylation site mutation in familiar advanced sleep phase syndrome. Science *291*, 1040–1043.

62. Eide, E.J., Woolf, M.F., Kang, H., Woolf, P., Hurst, W., Camacho, F., Vielhaber, E.L., Giovanni, A., and Virshup, D.M. (2005). Control of mammalian circadian rhythm by CKI epsilon regulated proteasome-mediated PER2 degradation. Mol. Cell Biol. *25*, 2795–2807.

63. Fustin, J.M., Kojima, R., Itoh, K., Chang, H.Y., Ye, S., Zhuang, B., Oji, A., Gibo, S., Narasimamurthy, R., Virshup, D., et al. (2018). Two δ transcripts regulated by m6A methylation code for two antagonistic kinases in the control of the circadian clock. Proc. Natl. Acad. Sci. USA *115*, 5980–5985.

64. Beg, Z.H., Allmann, D.W., and Gibson, D.M. (1973). Modulation of 3-hydroxy-3-methylglutaryl coenzyme: a reductase activity with cAMP and with protein fractions of rat liver cytosol. Biochem. Biophys. Res. Commun. *54*, 1362–1369.

65. Carlson, C.A., and Kim, K.H. (1973). Regulation of hepatic acetyl coenzyme A carboxylase by phosphorylation and dephosphorylation. J. Biol. Chem. *248*, 378–380.

66. Ingebritsen, T.S., Lee, H.S., Parker, R.A., and Gibson, D.M. (1978). Reversible modulation of the activities of both liver microsomal hydroxymethylglutaryl coenzyme A reductase and its inactivating enzyme. Evidence for regulation by phosphorylation-dephosphorylation. Biochem. Biophys. Res. Commun. *81*, 1268–1277.

67. Yeh, L.A., Lee, K.H., and Kim, K.H. (1980). Regulation of rat liver acetyl-CoA carboxylase. Regulation of phosphorylation and inactivation of acetyl-CoA carboxylase by the adenylate energy charge. J. Biol. Chem. *255*, 2308–2314.

68. Ferrer, A., Caelles, C., Massot, N., and Hegardt, F.G. (1985). Activation of rat liver cytosolic 3-hydroxy-3-methylglutaryl coenzyme A reductase kinase by adenosine 5'-monophosphate. Biochem. Biophys. Res. Commun. *132*, 497–504.

69. Carling, D., Zammit, V.A., and Hardie, D.G. (1987). A common bicyclic protein kinase cascade inactivates the regulatory enzymes of fatty acid and cholesterol biosynthesis. FEBS Lett. *223*, 217–222.

70. Munday, M.R., Campbell, D.G., Carling, D., and Hardie, D.G. (1988). Identification by amino acid sequencing of three major regulatory phosphorylation sites on rat acetyl-CoA carboxylase. Eur. J. Biochem. *175*, 331–338.

71. Carling, D., Clarke, P.R., Zammit, V.A., and Hardie, D.G. (1989). Purification and characterization of the AMP-activated protein kinase. Co-purification of acetyl-CoA carboxylase kinase and 3-hydroxy-3-methylglutaryl-Co-A reductase kinase activities. Eur. J. Biochem. *186*, 129–136.

72. Hardie, D.G. (2014). AMP-activated protein kinase: maintaining energy homeostasis at the cellular and whole-body levels. Annu. Rev. Nutr. *34*, 31–55.

73. López, M., Nogueiras, R., Tena-Sempere, M., and Diéguez, C. (2016). Hypothalamic AMPK: a canonical regulator of whole-body energy balance. Nat. Rev. Endocrinol. *12*, 421–432.

74. Hardie, D.G., Schaffer, B.E., and Brunet, A. (2016). AMPK: an energy-sensing pathway with multiple inputs and outputs. Trends Cell Biol. *26*, 190–201.

75. Herzig, S., and Shaw, R.J. (2018). AMPK: guardian of metabolism and mitochondrial homeostasis. Nat. Rev. Mol. Cell Biol. *19*, 121–135.

76. Liu, Y., Wang, T.V., Cui, Y., Li, C., Jiang, L., and Rao, Y. (2022). STE20 phosphorylation of AMPK related kinases revealed by biochemical purifications combined with genetics. J. Biol. Chem. *298*, 101928.

77. Hayasaka, N., Hirano, A., Miyoshi, Y., Tokuda, I.T., Yoshitane, H., Matsuda, J., and Fukada, Y. (2017). Salt-inducible kinase 3 regulates the mammalian circadian clock by destabilizing PER2 protein. eLife *6*, e24779.

78. Yu, J., Liu, H., Gao, R., Wang, T.V., Li, C., Liu, Y., Yang, L., Xu, Y., Cui, Y., Jia, C., et al. (2025). Calcineurin: An essential regulator of sleep revealed

by biochemical, chemical biological, and genetic approaches. Cell Chem. Biol. *32*, 157–173.e7.

79. Li, Y., Li, C., Liu, Y., Yu, J., Yang, J., Cui, Y., Wang, T.V., Li, C., Jiang, L., Song, M., and Rao, Y. (2023). Sleep need, the key regulator of sleep homeostasis, is indicated and controlled by phosphorylation of threonine 221 in salt-inducible kinase 3. Genetics *225*, iyad136.
80. Akashi, M., Tsuchiya, Y., Yoshino, T., and Nishida, E. (2002). Control of intracellular dynamics of mammalian period proteins by casein kinase I ε and CKIδ in cultured cells. Mol. Cell Biol. *22*, 1693–1703.
81. Kinoshita, E., Kinoshita-Kikuta, E., Takiyama, K., and Koike, T. (2006). Phosphate-binding tag, a new tool to visualize phosphorylated proteins. Mol. Cell. Proteomics *5*, 749–757.
82. Zhang, E.E., Liu, A.C., Hirota, T., Miraglia, L.J., Welch, G., Pongsawakul, P.Y., Liu, X., Atwood, A., Huss, J.W., 3rd, Janes, J., et al. (2009). A genome-wide RNAi screen for modifiers of the circadian clock in human cells. Cell *139*, 199–210.
83. Eide, E.J., Woolf, M.F., Kang, H., Woolf, P., Hurst, W., Camacho, F., Vielhaber, E.L., Giovanni, A., and Virshup, D.M. (2005). Control of mammalian circadian rhythm by CKIepsilon-regulated proteasome-mediated PER2 degradation. Mol. Cell Biol. *25*, 2795–2807.
84. Lowrey, P.L., Shimomura, K., Antoch, M.P., Yamazaki, S., Zemenides, P.D., Ralph, M.R., Menaker, M., and Takahashi, J.S. (2000). Positional syntenic cloning and functional characterization of the mammalian circadian mutation tau. Science *288*, 483–492.
85. Maier, B., Wendt, S., Vanselow, J.T., Wallach, T., Reischl, S., Oehmke, S., Schlosser, A., and Kramer, A. (2009). A large-scale functional RNAi screen reveals a role for CK2 in the mammalian circadian clock. Genes Dev. *23*, 708–718.
86. Iitaka, C., Miyazaki, K., Akaike, T., and Ishida, N. (2005). A role for glycogen synthase kinase-3 beta in the mammalian circadian clock. J. Biol. Chem. *280*, 29397–29402.
87. Honda, T., Fujiyama, T., Miyoshi, C., Ikkyu, A., Hotta-Hirashima, N., Kanno, S., Mizuno, S., Sugiyama, F., Takahashi, S., Funato, H., and Yanagisawa, M. (2018). A single phosphorylation site of SIK3 regulates daily sleep amounts and sleep need in mice. Proc. Natl. Acad. Sci. USA *115*, 10458–10463.
88. Meng, Q.J., Logunova, L., Maywood, E.S., Gallego, M., Lebiecki, J., Brown, T.M., Sládek, M., Semikhodskii, A.S., Glossop, N.R.J., Piggins, H.D., et al. (2008). Setting clock speed in mammals:: The CK1ε tau mutation in mice accelerates circadian pacemakers by selectively destabilizing PERIOD proteins. Neuron *58*, 78–88.
89. Kolodziej, P.A., and Young, R.A. (1991). Epitope tagging and protein surveillance. Methods Enzymol. *194*, 508–519.
90. Liu, Y., Wang, T.V., Cui, Y., Gao, S., and Rao, Y. (2022). Biochemical purification uncovers mammalian sterile 3 (MST3) as a new protein kinase for multifunctional protein kinases AMPK and SIK3. J. Biol. Chem. *298*, 101929.
91. Jagannath, A., Butler, R., Godinho, S.I.H., Couch, Y., Brown, L.A., Vasudevan, S.R., Flanagan, K.C., Anthony, D., Churchill, G.C., Wood, M.J.A., et al. (2013). The CRTC1-SIK1 pathway regulates entrainment of the circadian clock. Cell *154*, 1100–1111.
92. Hirota, T., Lee, J.W., Lewis, W.G., Zhang, E.E., Breton, G., Liu, X., Garcia, M., Peters, E.C., Etchegaray, J.P., Traver, D., et al. (2010). High-throughput chemical screen identifies a novel potent modulator of cellular circadian rhythms and reveals CKIalpha as a clock regulatory kinase. PLoS Biol. *8*, e1000559.
93. Edery, I., Zwiebel, L.J., Dembinska, M.E., and Rosbash, M. (1994). Temporal phosphorylation of the Drosophila period protein. Proc. Natl. Acad. Sci. USA *91*, 2260–2264.
94. Kloss, B., Price, J.L., Saez, L., Blau, J., Rothenfluh, A., Wesley, C.S., and Young, M.W. (1998). The Drosophila clock gene double-time encodes a protein closely related to human casein kinase Iepsilon. Cell *94*, 97–107.
95. Price, J.L., Blau, J., Rothenfluh, A., Abodeely, M., Kloss, B., and Young, M.W. (1998). double-time is a novel Drosophila clock gene that regulates PERIOD protein accumulation. Cell *94*, 83–95.
96. Vielhaber, E., Eide, E., Rivers, A., Gao, Z.H., and Virshup, D.M. (2000). Nuclear entry of the circadian regulator mPER1 is controlled by mammalian casein kinase I ε. Mol. Cell Biol. *20*, 4888–4899.
97. Kloss, B., Rothenfluh, A., Young, M.W., and Saez, L. (2001). Phosphorylation of period is influenced by cycling physical associations of double-time, period, and timeless in the Drosophila clock. Neuron *30*, 699–706.
98. Lee, C., Weaver, D.R., and Reppert, S.M. (2004). Direct association between mouse PERIOD and CKIε is critical for a functioning circadian clock. Mol. Cell Biol. *24*, 584–594.
99. Miyazaki, K., Nagase, T., Mesaki, M., Narukawa, J., Ohara, O., and Ishida, N. (2004). Phosphorylation of clock protein PER1 regulates its circadian degradation in normal human fibroblasts. Biochem. J. *380*, 95–103.
100. Nawathean, P., and Rosbash, M. (2004). The doubletime and CKII kinases collaborate to potentiate Drosophila PER transcriptional repressor activity. Mol. Cell *13*, 213–223.
101. Sathyanarayanan, S., Zheng, X., Xiao, R., and Sehgal, A. (2004). Posttranslational regulation of Drosophila PERIOD protein by protein phosphatase 2A. Cell *116*, 603–615.
102. Takano, A., Isojima, Y., and Nagai, K. (2004). Identification of mPer1 phosphorylation sites responsible for the nuclear entry. J. Biol. Chem. *279*, 32578–32585.
103. Cyran, S.A., Yiannoulos, G., Buchsbaum, A.M., Saez, L., Young, M.W., and Blau, J. (2005). The double-time protein kinase regulates the subcellular localization of the Drosophila clock protein period. J. Neurosci. *25*, 5430–5437.
104. Lin, J.M., Schroeder, A., and Allada, R. (2005). In vivo circadian function of casein kinase 2 phosphorylation sites in Drosophila PERIOD. J. Neurosci. *25*, 11175–11183.
105. Shirogane, T., Jin, J., Ang, X.L., and Harper, J.W. (2005). SCFbeta-TRCP controls clock-dependent transcription via casein kinase 1-dependent degradation of the mammalian period-1 (Per1) protein. J. Biol. Chem. *280*, 26863–26872.
106. Gallego, M., Kang, H., and Virshup, D.M. (2006). Protein phosphatase 1 regulates the stability of the circadian protein PER2. Biochem. J. *399*, 169–175.
107. He, Q., Cha, J., He, Q., Lee, H.C., Yang, Y., and Liu, Y. (2006). CKI and CKII mediate the FREQUENCY-dependent phosphorylation of the WHITE COLLAR complex to close the Neurospora circadian negative feedback loop. Genes Dev. *20*, 2552–2565.
108. Kim, E.Y., Ko, H.W., Yu, W., Hardin, P.E., and Edery, I. (2007). A DOUBLETIME kinase binding domain on the Drosophila PERIOD protein is essential for its hyperphosphorylation, transcriptional repression, and circadian clock function. Mol. Cell Biol. *27*, 5014–5028.
109. Nawathean, P., Stoleru, D., and Rosbash, M. (2007). A small conserved domain of Drosophila PERIOD is important for circadian phosphorylation, nuclear localization, and transcriptional repressor activity. Mol. Cell Biol. *27*, 5002–5013.
110. Blau, J. (2008). PERspective on PER phosphorylation. Genes Dev. *22*, 1737–1740.
111. Chiu, J.C., Vanselow, J.T., Kramer, A., and Edery, I. (2008). The phospho-occupancy of an atypical SLIMB-binding site on PERIOD that is phosphorylated by DOUBLETIME controls the pace of the clock. Genes Dev. *22*, 1758–1772.
112. Etchegaray, J.P., Machida, K.K., Noton, E., Constance, C.M., Dallmann, R., Di Napoli, M.N., DeBruyne, J.P., Lambert, C.M., Yu, E.A., Reppert, S.M., and Weaver, D.R. (2009). Casein kinase 1 delta regulates the pace of the mammalian circadian clock. Mol. Cell Biol. *29*, 3853–3866.

113. Ko, H.W., Kim, E.Y., Chiu, J., Vanselow, J.T., Kramer, A., and Edery, I. (2010). A hierarchical phosphorylation cascade that regulates the timing of PERIOD nuclear entry reveals novel roles for proline-directed kinases and GSK-3beta/SGG in circadian clocks. J. Neurosci. *30*, 12664–12675.

114. Schmutz, I., Wendt, S., Schnell, A., Kramer, A., Mansuy, I.M., and Albrecht, U. (2011). Protein phosphatase 1 (PP1) is a post-translational regulator of the mammalian circadian clock. PLoS One *6*, e21325.

115. Chiu, J.C., Ko, H.W., and Edery, I. (2011). NEMO/NLK phosphorylates PERIOD to initiate a time-delay phosphorylation circuit that sets circadian clock speed. Cell *145*, 357–370.

116. Lee, H.M., Chen, R., Kim, H., Etchegaray, J.P., Weaver, D.R., and Lee, C. (2011). The period of the circadian oscillator is primarily determined by the balance between casein kinase 1 and protein phosphatase 1. Proc. Natl. Acad. Sci. USA *108*, 16451–16456.

117. Uchida, Y., Osaki, T., Yamasaki, T., Shimomura, T., Hata, S., Horikawa, K., Shibata, S., Todo, T., Hirayama, J., and Nishina, H. (2012). Involvement of stress kinase mitogen-activated protein kinase kinase 7 in regulation of mammalian circadian clock. J. Biol. Chem. *287*, 8318–8326.

118. Garbe, D.S., Fang, Y., Zheng, X., Sowcik, M., Anjum, R., Gygi, S.P., and Sehgal, A. (2013). Cooperative interaction between phosphorylation sites on PERIOD maintains circadian period in Drosophila. PLoS Genet. *9*, e1003749.

119. Kaasik, K., Kivimae, S., Allen, J.J., Chalkley, R.J., Huang, Y., and Baer, K. (2013). Glucose Sensor O-GlcNAcylation coordinates with phosphorylation to regulate circadian Clock. Cell Metab. *17*, 291–302.

120. Maywood, E.S., Chesham, J.E., Smyllie, N.J., and Hastings, M.H. (2014). The Tau mutation of casein kinase 1epsilon sets the period of the mammalian pacemaker via regulation of Period1 or Period2 clock proteins. J. Biol. Rhythms *29*, 110–118.

121. Marzoll, D., Serrano, F.E., Shostak, A., Schunke, C., Diernfellner, A.C.R., and Brunner, M. (2022). Casein kinase 1 and disordered clock proteins form functionally equivalent, phospho-based circadian modules in fungi and mammals. Proc. Natl. Acad. Sci. USA *119*, e2118286119.

122. Levine, D.C., Reeh, R.H., McMahon, T., Mandrup-Poulsen, T., Fu, Y.-H., and Ptáček, L.J. (2025). Unsaturated fat alters clock phosphorylation to align rhythms to the season in mice. Science *390*, eadp3065.

123. Lizcano, J.M., Göransson, O., Toth, R., Deak, M., Morrice, N.A., Boudeau, J., Hawley, S.A., Udd, L., Mäkelä, T.P., Hardie, D.G., and Alessi, D.R. (2004). LKB1 is a master kinase that activates 13 kinases of the AMPK subfamily, including MARK/PAR-1. Embo J *23*, 833–843.

124. Jaleel, M., McBride, A., Lizcano, J.M., Deak, M., Toth, R., Morrice, N.A., and Alessi, D.R. (2005). Identification of the sucrose non-fermenting related kinase SNRK, as a novel LKB1 substrate. FEBS Lett. *579*, 1417–1423.

125. Thirugnanam, K., and Ramchandran, R. (2020). SNRK: a metabolic regulator with multifaceted role in development and disease. Vessel Plus *4*, 26.

126. Kim, C.L., Lim, S.B., Choi, S.H., Kim, D.H., Sim, Y.E., Jo, E.H., Kim, K., Lee, K., Park, H.S., Lim, S.B., et al. (2024). The LKB1–TSSK1B axis controls YAP phosphorylation to regulate the Hippo–YAP pathway. Cell Death Dis. *15*, 76.

127. Wang, J.W., Imai, Y., and Lu, B. (2007). Activation of PAR-1 kinase and stimulation of tau phosphorylation by diverse signals require the tumor suppressor protein LKB1. J. Neurosci. *27*, 574–581.

128. Choi, S., Lim, D.S., and Chung, J. (2015). Feeding and Fasting Signals Converge on the LKB1-SIK3 Pathway to Regulate Lipid Metabolism in Drosophila. PLoS Genet. *11*, e1005263.

129. Sanjana, N.E., Shalem, O., and Zhang, F. (2014). Improved vectors and genome-wide libraries for CRISPR screening. Nat. Methods *11*, 783–784.

130. Zhang, E.E., Liu, A.C., Hirota, T., Miraglia, L.J., Welch, G., Pongsawakul, P.Y., Liu, X., Atwood, A., Huss, J.W., Janes, J., et al. (2009). A Genome-wide RNAi Screen for Modifiers of the Circadian Clock in Human Cells. Cell *139*, 199–210.

STAR★METHODS

KEY RESOURCES TABLE

REAGENT or RESOURCE	SOURCE	IDENTIFIER
Antibodies		
anti-PER2 pS662	Abcam	Cat# ab206377; RRID:AB_3713265
anti-PER2	Abcam	Cat# ab227727; RRID:AB_3718162
anti-CK1δ	Abcam	Cat# ab85320; RRID: AB_1860174
anti-CK1ε	Abcam	Cat# ab1796; RRID: AB_10804849
anti-MARK1	Abcam	Cat# ab154357; AB_3720986
anti-MARK3	Abcam	Cat# ab52626; RRID: AB_881139
anti-phospho-MARK Family (Activation Loop)	Cell Signaling Technology	Cat# 4836; RRID: AB_2140607
anti-MBP Tag	Cell Signaling Technology	Cat# 2396; RRID: AB_2140060
anti-GFP	Cell Signaling Technology	Cat# 2555; RRID: AB_10692764
anti-JNK	Cell Signaling Technology	Cat# 9252; RRID: AB_2250373
anti-phospho-JNK	Cell Signaling Technology	Cat# 9251; RRID: AB_331659
anti-ERK1/2	Cell Signaling Technology	Cat# 4695; RRID: AB_390779
anti-phospho-ERK	Cell Signaling Technology	Cat# 4370; RRID: AB_2315112
anti-GSK3β	Cell Signaling Technology	Cat# 12456; RRID: AB_2636978
anti–GSK3β pS9	Cell Signaling Technology	Cat# 14332; RRID: AB_2798453
anti-β actin	Santa Cruz Biotechnology	Cat# sc-47778; RRID: AB_626632
anti-HA	Santa Cruz Biotechnology	Cat# sc7392; RRID: AB_627809
anti-MARK2	Santa Cruz Biotechnology	Cat# sc365405; RRID: AB_10841762
anti-Flag M2 HRP conjugated	Sigma-Aldrich	Cat# A8592; RRID: AB_439702
anti-MARK4	Thermo Fisher Biotechnology	Cat# PA5104542; RRID: AB_2853482
Bacterial and virus strains		
E. coli: BL21 (DE3)	Transgen	Cat# CD601-02
Chemicals, peptides, and recombinant proteins		
phosphatase inhibitor cocktail 2	Sigma-Aldrich	Cat# P5726
phosphatase inhibitor cocktail 3	Sigma-Aldrich	Cat# P0044
Luciferin-Na	Thermofisher	Cat# 88292
protease inhibitor cocktail tablets	Sigma-Aldrich	Cat# 04693132001
B-27 Supplement	Thermofisher	Cat# 17504044
Sodium bicarbonate (7.5%)	Thermofisher	Cat# 25080094
HEPES-NaOH (pH=7.0)	Thermofisher	Cat# 15630080
Lipo3000	Thermofisher	Cat# L3000-015
1×PBS pH=7.4	Thermofisher	Cat# 10010049
Penicillin-Streptomycin	Thermofisher	Cat# 15070-063
FBS	Thermofisher	Cat# 10099-141C
Phos-tag™ Acrylamide	Fujifilm Wako	AAL-107
Experimental models: Cell lines		
Human: HEK293T	ATCC; authenticated	Cat# CRL-3216
D15 (Per2::dLuc U2OS) cells	Gifted from Dr. Eric Zhang; authenticated	N/A
Experimental models: Organisms/strains		
Mouse: *CK1δ*^{flox}	Jackson Laboratories	RRID:IMSR_JAX:010487
Mouse: *Mark3* knockout	GemPharmatech (China)	RRID:IMSR_GPT:T029467
Mouse: *Tssk2* knockout	this paper	N/A

(*Continued on next page*)

Continued

REAGENT or RESOURCE	SOURCE	IDENTIFIER
Mouse: *Tssk1-Tssk2*^{flox}	this paper	N/A
Mouse: *Mark2*^{flox}	this paper	N/A
Mouse: *Mark3*^{flox}	this paper	N/A
Mouse: *Mark4*^{flox}	this paper	N/A
Oligonucleotides		
See Table S2 for Oligonucleotide sequences	this paper	N/A
Recombinant DNA		
pMDG.2	pMD2.G was a gift from Didier Trono	Addgene: Cat# 12259
psPAX2	psPAX2 was a gift from Didier Trono	Addgene: Cat# 12260
LentiCRISPRV2-Cas9	Sanjana et al.[129]	Addgene: Cat# 52961
pCDNA3.1-3xFlag-PER2	this paper	N/A
pCDNA3.1-3xFlag-PER2 S662A	this paper	N/A
pCDNA3.1-3xFlag-PER2 S662D	this paper	N/A
pCDNA3.1-HA-mouse PER2	this paper	N/A
pCDNA3.1-HA-mouse PER2 S659A	this paper	N/A
pCDNA3.1-HA-mouse PER2 S659D	this paper	N/A
pCDNA3.1-3xFlag-PER2 556-771	this paper	N/A
pCDNA3.1-3xFlag-PER2 556-771 S662A	this paper	N/A
pCDNA3.1-3xFlag-EF2K	this paper	N/A
pCDNA3.1-3xFlag-IKKα	this paper	N/A
pCDNA3.1-3xFlag-TLK1	this paper	N/A
pCDNA3.1-3xFlag-TNN3K	this paper	N/A
pCDNA3.1-3xFlag-MAP3K7	this paper	N/A
pCDNA3.1-3xFlag-TNK1	this paper	N/A
pCDNA3.1-3xFlag-CK1α1	this paper	N/A
pCDNA3.1-3xFlag-CK1α2	this paper	N/A
pCDNA3.1-3xFlag-CK1δ	this paper	N/A
pCDNA3.1-3xFlag-CK1ε	this paper	N/A
pCDNA3.1-3xFlag-CK1γ1	this paper	N/A
pCDNA3.1-3xFlag-CK1γ2	this paper	N/A
pCDNA3.1-3xFlag-CK1γ3	this paper	N/A
pCDNA3.1-3xFlag-TSSK1	this paper	N/A
pCDNA3.1-3xFlag-TSSK2	this paper	N/A
pCDNA3.1-3xFlag-TSSK3	this paper	N/A
pCDNA3.1-3xFlag-TSSK4	this paper	N/A
pCDNA3.1-3xFlag-TSSK6	this paper	N/A
pCDNA3.1-3xFlag-GSK-3β	this paper	N/A
pCDNA3.1-3xFlag-MKNK1	this paper	N/A
pCDNA3.1-3xFlag-SRC	this paper	N/A
pCDNA3.1-3xFlag-RSK2	this paper	N/A
pCDNA3.1-3xFlag-MARK1	this paper	N/A
pCDNA3.1-3xFlag-MARK2	this paper	N/A
pCDNA3.1-3xFlag-MARK3	this paper	N/A
pCDNA3.1-3xFlag-MARK4	this paper	N/A
pCDNA3.1-3xFlag-MARK2 T208A	this paper	N/A
pCDNA3.1-3xFlag-MARK2 T208E	this paper	N/A
pCDNA3.1-3xFlag-MARK3 T211A	this paper	N/A
pCDNA3.1-3xFlag-MARK3 T211E	this paper	N/A
pCDNA3.1-3xFlag-mouse-MARK2	this paper	N/A

(*Continued on next page*)

Continued

REAGENT or RESOURCE	SOURCE	IDENTIFIER
pCDNA3.1-3xFlag-mouse-MARK2 T208A	this paper	N/A
pCDNA3.1-3xFlag-mouse-MARK2 T208E	this paper	N/A
pCDNA3.1-3xFlag-mouse-MARK3	this paper	N/A
pCDNA3.1-3xFlag-mouse-MARK3 T211A	this paper	N/A
pCDNA3.1-3xFlag-mouse-MARK3 T211E	this paper	N/A
pCDNA3.1-3xFlag-AMPKα1	this paper	N/A
pCDNA3.1-3xFlag-AMPKα2	this paper	N/A
pCDNA3.1-3xFlag-SIK1	this paper	N/A
pCDNA3.1-3xFlag-SIK2	this paper	N/A
pCDNA3.1-3xFlag-SIK3	this paper	N/A
pCDNA3.1-3xFlag-BRSK1	this paper	N/A
pCDNA3.1-3xFlag-BRSK2	this paper	N/A
pCDNA3.1-3xFlag-NUAK1	this paper	N/A
pCDNA3.1-3xFlag-NUAK2	this paper	N/A
pCDNA3.1-3xFlag-SNRK	this paper	N/A
pCDNA3.1-3xFlag-NIM1	this paper	N/A
pCDNA3.1-3xFlag-HUNK1	this paper	N/A
pCDNA3.1-HA-MAR2	this paper	N/A
pCDNA3.1-HA-MAR3	this paper	N/A
pCDNA3.1-HA-PER2	this paper	N/A
pCDNA3.1-HA-PER2 1-438	this paper	N/A
pCDNA3.1-HA-PER2 321-557	this paper	N/A
pCDNA3.1-HA-PER2 471-788	this paper	N/A
pCDNA3.1-HA-PER2 717-1255	this paper	N/A
pCDNA3.1-HA-PER2 321-717 Δ438-497	this paper	N/A
pCDNA3.1-HA-PER2 321-717 Δ498-557	this paper	N/A
pLVX-3xFlag-MARK1	this paper	N/A
pLVX-3xFlag-MARK2	this paper	N/A
pLVX-3xFlag-MARK3	this paper	N/A
pLVX-3xFlag-MARK4	this paper	N/A
Software and algorithms		
GraphPad Prism 8.0	GraphPad Software Inc.	https://www.graphpad.com/
ImageJ	NIH	https://imagej.nih.gov/ij/
Lumicycle Analysis	Lumicycle Analysis	Version 2.53
Image Lab	BioRad	https://www.bio-rad.com/en-us/product/image-lab-software?ID=KRE6P5E8Z
Other		
Nitrocellulose membrane	Sigma-Aldrich	Cat# HATF00010
Low-Profile Wireless Running Wheel	Med Associates Inc	Cat# ENV-047
HiTrap SP HP, 5 ml	Cytiva Inc	Cat# 17115201
HiTrap Blue HP, 5 ml	Cytiva Inc	Cat# 17041301
HiTrap Heparin HP, 5 ml	Cytiva Inc	Cat# 17040703
HiTrap Q HP, 1 ml	Cytiva Inc	Cat# 17115301
HAP (CHT Ceramic Hydroxyapatite, Type II, 20 μm)	Bio-rad	Cat# 1572000
Superdex 200 Increase 10/300 GL	Cytiva Inc	Cat# 28990944
HisTrap HP, 5 mL	Cytiva Inc	Cat# 17524801
MBPTrap HP, 5 ml	Cytiva Inc	Cat# 28918779
Amicon® Ultra Centrifugal Filter, 10 kDa MWCO	Sigma-Aldrich	UFC901096

EXPERIMENTAL MODEL AND STUDY PARTICIPANT DETAILS

Cell lines

HEK293T (fetal, female) cell line was purchased from ATCC (CRL-3216). Authentication information for HEK293T cell line is available at the website. Cells were cultured in DMEM medium supplemented with 10% FBS and 1% Penicillin/Streptomycin at 37°C with 5% CO_2. Cells were passaged every 2 days. D15 (Per2::dLuc U2OS) cells were a gift from Professor Eric Erquan Zhang (National Institute of Biological Sciences, Beijing).[130] The parental U2OS cell line was derived from a 15-year-old female patient with osteosarcoma and has been authenticated by ATCC. Cells were maintained in DMEM supplemented with 10% FBS, 1% penicillin/streptomycin, and MEM nonessential amino acids. All cell lines used in this study were confirmed to be mycoplasma-free prior to experimentation.

Animals

All experimental procedures were performed in accordance with the guidelines and were approved by the Animal Care and Use Committee (ACUC) of Chinese Institute for Brain Research (CIBR), Beijing. Mutant mice and wt littermates were maintained on a C57BL/6N background. Mice were maintained on a 12 h light/dark cycle in a temperature- and humidity-controlled facility with *ad libitum* access to food and water.

METHOD DETAILS

Detection of phosphorylation by phos-tag

Phos-tag SDS-PAGE was performed according to the manufacturer's protocol (Phos-tag Acrylamide AAL-107), with a minor modification that the final concentration of phos-tag in the gel was 25 μM. Phos-tag binds to phosphate groups on proteins slowed down their migration during SDS-PAGE.[81] Shifted bands corresponding to phosphorylated hPER2 fragments were detected by immunoblotting with an anti-FLAG- horseradish peroxidase (HRP) antibody.

Expression and purification of recombinant proteins

cDNAs were cloned into the pET-28a vector with designated tags. For recombinant protein expression, the plasmids were transformed into *E. coli* BL21 (DE3) cells. A single colony was inoculated into 5 mL of Luria-Bertani (LB) broth containing 50 μg/mL kanamycin and cultured overnight at 37°C with shaking at 220 rpm. The overnight culture was diluted 1:1000 into fresh LB medium with kanamycin and grown at 37°C until the optical density at 600 nm (OD_{600}) reached 0.6–0.8. Protein expression was induced by adding 0.5 mM isopropyl β-d-1-thiogalactopyranoside, and the culture was incubated at 18°C for 16 h with continuous shaking. Cells were harvested and lysed in Ni^{2+} binding buffer (300 mM NaCl, 20 mM Tris-HCl, pH7.5) supplemented with protease inhibitors, and lysed by sonication, followed by centrifugation at 14,000 rpm for 30 min. Recombinant proteins were purified by Ni^{2+} affinity columns and stored at -80°C. For proteins used as substrates, the tag was not removed. For a protein used as the kinase, the fusion protein was incubated with His-tagged TEV protease to release the untagged kinase protein from the myelin basic protein (MBP) tag and GFP-8×His tag. The cleavage reaction mixture was subsequently passed over a Ni-NTA column to remove the GFP-8×His tag, the TEV protease and uncut fusion protein. The flow-through, containing the untagged protein and MBP tag, was collected and further purified by MBP affinity chromatography to remove any residual MBP-containing fragments. The final purified, untagged protein was buffer-exchanged into Buffer A (20 mM HEPES pH 7.5, 150 mM NaCl, 1 mM DTT) using centrifugal filtration and flash-frozen in liquid nitrogen for storage at -80°C.

Purification of MARK 2 and 3 from HEK293T cells

500 ml HEK293T cell lysates (10 mg/ml) were purified by sequentially connected chromatography steps as diagramed in Figure 1C. Purification was performed at 4°C with an AKTA Purifier 10 FPLC system (GE Healthcare). Cell lysates were loaded onto 10 ml SP HP columns pre-equilibrated with buffer A. Columns were eluted with a linear gradient of 20 CV buffer A from 0 to 600 mM NaCl. 20 fractions were collected, and aliquots of 0.5 ml of each fraction were dialyzed against buffer A, followed by *in vitro* PER2 S662 phosphorylation assay. Active fractions (7 and 8) from SP HP columns (Figure 1D) were pooled and loaded 10 ml Blue HP columns and eluted with a linear gradient of 0 to 3000 mM NaCl in 20 CV buffer A. Active fractions (7 to 11, 1050-1650 mM NaCl) from the Blue column (Figure 1E) were loaded on 10 ml Heparin HP columns and were eluted with a linear gradient of 0 to 600 mM NaCl in 20 CV buffer A. Active fractions (9 to 13,270-330 mM NaCl) from the Heparin HP column (Figure 1F) were loaded on 10 ml Q HP columns and eluted with a linear gradient of 0 to 600 mM NaCl in 20 CV buffer A. Active fractions (4 to 7,120-210 mM NaCl) from the Q HP column (Figure 1G) were loaded on 1 ml HAP (Hydroxyapatite column (Bio-Rad)) columns, eluted with a linear gradient of K_2PO_4 buffer from 0 to 300 mM. Active fractions (11 and 12, 150-180 mM K_2PO_4) from the HAP column (Figure 1H) were concentrated to 0.5 ml, and loaded onto Superdex 200 10/300 column, and eluted with 200 mM NaCl in Buffer A. Fractions from Superdex 200 10/300 column (Figure 1I) were assayed for PER2 S662 phosphorylation activity, and active fractions (11 and 12, 200 mM NaCl) were subjected to MS analysis.

In vitro kinase assay

Purified fractions (10 μl) or recombinant kinases (0.5 μg) were incubated with 1 μg substrates at 37°C for 1hr in buffer A (20 mM HEPES,10 mM KCl,1.5 mM MgCl2,1 mM EDTA,1 mM EGTA,1 mM DTT, 1x protease inhibitor cocktail, 1x phosphatase inhibitor II

and 1x phosphatase inhibitor III) with 1 mM ATP (pH7.5) in a total volume of 20 μl. Reactions were terminated by heating at 95°C with the protein loading buffer and analyzed by immunoblotting.

Calculation of the Michaelis-Menten constant

0.2 μg recombinant kinase was incubated with the substrate at multiple concentrations at 37°C for 20 mins in buffer A (20 mM HEPES,10 mM KCl,1.5 mM $MgCl_2$,1 mM EDTA,1 mM EGTA,1 mM DTT, 1xprotease inhibitor cocktail, 1xphosphatase inhibitor II and 1x phosphatase inhibitor III). Reactions were terminated by heating at 95°C with the protein loading buffer and analyzed by Western blots. Western blots were quantitated by the ImageJ software and Km calculated by the GraphPad Prism software.

Protein stability assay

HEK293T cells were transfected with PER2 WT or S662G mutant or co-transfected with MARK2 for 24 hrs. Transfected cells were treated with DMSO or 200 mM cycloheximide (CHX) before harvesting at the indicated time points. Equal extracts were subjected to immunoblot analysis with the indicated antibodies, with actin as a loading control. Western blots were quantitated by the ImageJ software, and protein half-life was calculated by the GraphPad Prism software.

Generation of KO cell lines

Knockout HEK cells deficient in *MARK 1* to *4* were generated by CRISPR/Cas9-mediated gene targeting. Briefly, two sequentially connected guide sequences targeting the indicated gene were inserted into the lentiCRISPRv2 puro vector. The lentiCRISPRv2 plasmids were transfected into cells with Lipofectamine 3000 (Thermo Fisher Scientific, L3000015), followed by puromycin selection. Single clones were selected from 96-well plates by limited dilution. The success of gene-targeting single clone cells was confirmed by immunoblotting with appropriate antibodies.

Circadian rhythm analysis of D15 cells

For rhythm recording, cells were passaged onto 10 mm x 35 mm dishes and synchronized by replacing the medium with XM medium (1× DMEM(Gibco), 1× B27 supplement (Gibco), 4.2 mM $NaHCO_3$ (Gibco), 10 mM HEPES (Gibco), 100 U/ml penicillin and streptomycin (Gibco) and 1 mM luciferin (Gibco)) when the confluence rate was 100%. The dishes were sealed with high vacuum grease (Dow Corning) and microscope cover glass (Fisherbrand) and bioluminescence was continuously recorded in a LumiCycle (Actimetrics) placed within an incubator (37°C, 5% CO_2) for approximately 3-4 days. Period lengths of bioluminescence rhythms were analysed using Lumicycle analysis software.

Generation of PER2 S662G mutant D15 cells with prime editing 7

The *PER2 S662G* mutation was introduced into D15 cells using the PE7 system. PegRNA and sgRNA were designed by the online tool (http://pegfinder.sidichenlab.org/). The spacer sequence of pegRNA is GCTCGCTGGCACTGCCGGGCA, and the sequence of sgRNA is CTTGTCTCCCACATGGACGA. The RTT and PBS sequences of pegRNA are ACACCCTCTGCCTTGCCCGGCAGTGCCAG. After transfected with plasmids of PE7-EGFP and hML1dn-cherry for 1 day, D15 cells expressing both EGFP and cherry fluorescence were sorted by FACS and cultured in a 35mm dish for another 2 days. For the editing step, 3.75μg of PER2 S662G pegRNA and 1.25μg of sgRNA plasmid were transfected, and cells were cultured for 3 days to edit the target site, followed by puromycin selection. Single clones were selected from 96-well plates by limited dilution. *PER2 S662G* point mutation cells were confirmed through PCR sequencing.

Mouse stocks

CK1δ^{flox} mice (RRID:IMSR_JAX:010487) were a gift from Prof. Ying Xu of Suzhou University. *Mark3* (RRID:IMSR_GPT:T029467) KO mice were purchased from GemPharmatech (Nanjing, China). *Tssk2* KO mice and *Tssk1-Tssk2* conditional double KO mice (*Tssk1-Tssk2*^{flox}), *Mark2* conditional KO mice (*Mark2*^{flox}), Mark3 conditional KO mice (*Mark3*^{flox}) and *Mark4* conditional KO mice (*Mark4*^{flox}) mice were created with the CRISPR/Cas9 system by the Genetic Manipulation Core of CIBR (Figures S4 and S11).

Wheel running assays of circadian rhythms in mice

All experimental procedures were approved by the ACUC of the CIBR. Male mice aged 11 to 24 were individually housed in a cage. Food and water were delivered *ad libitum*. The low-profile wireless running wheel system (Med Associates company, ENV-047) was used to record the circadian rhythm. Mice were acclimated to a standard light cycle (12D:12D) for 14 days, followed by 21 days of constant darkness (DD). Activity pattern diagrams of mice for every 10 mins were created and analyzed. Circadian period length was extracted from the DD phase of the wheel running activity records by X^2 periodogram analysis.

QUANTIFICATION AND STATISTICAL ANALYSIS

Statistical analysis was conducted with GraphPad Prism 8.0 (GraphPad Software). All statistical details can be found in the figure legends. Data were presented as mean ± SEM unless otherwise stated. Normality of the data was assessed using the Shapiro-Wilk normality test. If the data met the assumptions of normality and equal variance, parametric tests were applied; otherwise,

nonparametric alternatives were used (Kruskal-Wallis test). For detaile, unpaired, two-tailed Student's t test was used for comparisons between two groups; one-way ANOVA followed by Dunnett's multiple comparisons test was used for comparisons of multiple groups against control group; one-way ANOVA followed by Tukey's multiple comparisons test was used for comparisons between all groups; two-way ANOVA followed by Sidak's multiple comparisons was used to compare the differences between different groups with different treatments. ImageJ software was used for densitometry analysis of western blotting and data plotted in GraphPad Prism, data were presented as mean ± SEM and points reflect quantification from n = 3 biological replicates. Asterisks denote statistical significance: *p< 0.05, **p< 0.01, ***p< 0.001, **** p< 0.0001. Unless otherwise indicated, n represents the number of biologically independent samples, animals, or replicate experiments, as detailed in each figure legend. All experiments were performed at least three times, and representative data were shown. A complete summary of the sample sizes (n) for each experimental group in every figure panel is provided in Tables S3 and S4.